BA 243

E.ON Energy Research Center | RWTH AACHEN UNIVERSITY

Bachelor's Thesis

Development of a Hierarchical Multi-Agent-System for Operational Optimization of Energy Systems

Entwicklung eines Hierarchischen Multi-Agenten-Systems für die Betriebsoptimierung von Energiesystemen

Aachen, September 2020

Abdullah Tokmak
Matriculation number: 368331

Supervisors:
Alexander Kümpel, M.Sc.
Univ.-Prof. Dr.-Ing. Dirk Müller

The present work was submitted to the:
E.ON Energy Research Center | ERC
Institute for Energy Efficient Buildings and Indoor Climate | EBC
Mathieustrasse 10, 52074 Aachen, Germany

Abstract

One of the most significant goals in the course of climate protection is to reduce energy consumption. Since a large part of the energy consumption takes place in buildings, a significant potential for energy savings lies in the area of building energy systems. One reason for the high energy consumption in buildings is often inefficient control. However, promising control strategies to reduce energy consumption are computationally complex. To reduce the computational complexity, it is possible to divide the global system into subsystems. Each subsystem contains components, which are controlled by agents. The agents inside a subsystems are regulated by a sub-coordinator. The interaction between the sub-coordinators is handled by a coordinator. The presence of coordinating instances leads to a hierarchy within the multi-agent-system.

In this thesis, a hierarchical multi-agent-system is developed and applied to a building energy system to ensure efficient operation. Efficient operation is defined as an operation, which minimizes energy costs, control deviation, CO_2-emissions, and lifetime-reduction of the components. These criteria are considered by the agents when creating their cost functions. Every agent transfers its operational cost to its sub-coordinator. The cost function of the sub-coordinator is derived by the sum of the costs of its agents. By determining the cost-minimizing set-variables for the agents, the sub-coordinator aims to minimize its cost function to enable an optimal operation of its subsystem. The cost function of the coordinator consists of the sum of the operational costs of all sub-coordinators. The coordinator's objective is to initiate an operational optimization of the global system by specifying the optimal coupling variables of the subsystems.

The developed agent-based system is applied to the E.ON ERC main building energy system in a simulation. The introduced operational optimization is evaluated by considering control deviation, energy consumption, and energy costs. The attained results show, that the operational optimization can control the set-temperature more precisely when compared to a benchmark simulation. Moreover, the optimized operation leads to a simulation with 15 % lessened energy costs.

Zusammenfassung

Eines der wichtigsten Ziele im Zuge des Klimaschutzes ist die Reduzierung des Energieverbrauchs. Da ein großer Teil des Energieverbrauchs in Gebäuden stattfindet, haben Gebäudeenergiesysteme ein hohes Potential für Energieeinsparungen. Ein Grund für den hohen Energieverbrauch von Gebäudeenergiesystemen ist oftmals eine ineffiziente Regelung. Regelungen, die zu einem effizienten Betrieb führen, weisen jedoch einen hohen Implementierungs- und Rechenaufwand auf. Deshalb wird das Gesamtsystem in Subsysteme unterteilt. Jedes Subsystem enthält Komponenten, die von Agenten geregelt werden. Die Agenten innerhalb eines Subsystems werden von einem Sub-Koordinator gesteuert. Die Interaktion zwischen den Sub-Koordinatoren wird von einem Koordinator optimiert. Aufgrund der koordinierenden Instanzen wird das System als ein hierarchisches Multi-Agenten-System bezeichnet.

In dieser Arbeit wird ein hierarchisches Multi-Agenten-System entwickelt und auf ein Energiesystem angewandt, um einen effizienten Betrieb zu gewährleisten. Ein effizienter Betrieb minimiert Energiekosten, Regelabweichungen, CO_2-Emissionen und die Abnutzung der Komponenten. Diese Kriterien werden von den Agenten beim Erstellen ihrer Kostenfunktionen berücksichtigt. Jeder Agent übergibt seine Betriebskosten an seinen Sub-Koordinator. Die Kostenfunktion des Sub-Koordinators ergibt sich aus der Summe der Kosten seiner Agenten. Durch die Bestimmung der kostenminimierenden Sollwerte der Agenten, leitet der Sub-Koordinator einen optimalen Betrieb innerhalb des Subsystems ein. Die Kostenfunktion des Koordinators ergibt sich aus der Summe der Kosten aller Sub-Koordinatoren. Das Ziel des Koordinators ist es, einen optimalen Betrieb des globalen Systems einzuleiten, indem er die kostenminimierenden Kopplungsvariablen der Subsysteme bestimmt.

Das entwickelte System wird in einer Simulation auf das Energiesystem des E.ON ERC-Hauptgebäudes angewandt. Die Betriebsoptimierung wird unter Berücksichtigung der Regelgüte, des Energieverbrauchs und der Energiekosten bewertet. Die Ergebnisse zeigen, dass die Betriebsoptimierung im Vergleich zu einer Referenzregelung eine bessere Einhaltung der Solltemperatur gewährleistet. Außerdem führt der optimierte Betrieb zu einer Simulation mit 15 % geringeren Energiekosten.

Table of Contents

Nomenclature

Symbols and Units

Symbol	Meaning	Unit
a	pre-factor (constraint)	—
A_{cover}	cover surface	m^2
A_{shell}	shell surface	m^2
b	dimension (constraint)	—
$B_{10,d}$	expected cycles in the lifespan	cycles
$b_{el,CHP}$	electrical benefit-factor of the CHP	MU/(kWh)
c	pre-factor (constraint)	1/(MU)
c_{CO2}	cost-factor CO_2	MU/(t)
c_{el}	cost-factor electricity	MU/(kWh)
c_{heat}	cost-factor heat	MU/(kWh)
c_{MTA}	cost per multi-turn-actuator	MU
c_p	heat capacity (isobar)	kg/(kWK)
c_v	heat capacity (isochor)	kg/(kWK)
C_{prod}	productivity factor	—
$cost_{cons}$	constraint costs	MU
$cost_{operation}$	operational costs	MU
$cost_{em}$	emission costs	MU
$cost_{en}$	energy costs	MU
$cost_{lr}$	lifetime-reduction costs	MU
$cost_{th}$	thermal costs	MU
d	dimension (constraint)	—
e	control deviation	—
$f_{CO2,heat}$	emission factor heat	t/(kWh)
$f_{CO2,el}$	emission factor electricity	t/(kWh)
G	annual income	MU
k	thermal transmittance coefficient	$kW/(m^2K)$
m	mass	kg

Continued on the next page

Symbols and Units

Symbol	Meaning	Unit
$\dot{m}$	mass flow	kg/(s)
n_{MTA}	number of multi-turn-actuators	—
N_c	control horizon	—
N_p	prediction horizon	—
N_{fev}	number of function evaluations	—
P_{met}	probability of acceptance (metropolis criterion)	—
Q	heat	kJ
$\dot{Q}$	heat flow	kW
t	time	s
t_{cycle}	cycle time	s
$T_{10,d}$	expected lifespan	years
T	temperature	K
$\overline{T}$	mean temperature	K
T_{act}	actual temperature	K
T_{set}	set temperature	K
T_{met}	temperature parameter (metropolis criterion)	—
t	time	s
U	internal energy	kJ
V	volume	m^3
W	electrical energy	kJ
$\dot{W}$	power	kW

Greek Symbols

Symbol	Meaning	Unit
δt	time-interval	min
ΔT_{dev}	actual temperature deviation of the consumer	K
δT_{dev}	allowed temperature deviation of the consumer	K
η_{cost}	cost efficiency of the HTS	—
$\eta_{th,boiler}$	thermal efficiency of the boiler	—
$\eta_{th,CHP}$	thermal efficiency of the CHP	—

Continued on the next page

Greek Symbols

Symbol	Meaning	Unit
$\eta_{el,CHP}$	electrical efficiency of the CHP	—
ϵ_{HP}	coefficient of performance of the heat pump	—
ρ	density	$kg/(m^3)$

Indices and Abbreviations

Symbol	Meaning
0	initial state
act	actual
approx	approximated
B	boiler
BH	basin-hopping
BO	Bayesian optimization
C	consumer
cfg	cost-function-generator
CHP	combined heat and power
CO	condenser
conv	convective
CO_2	carbon dioxide
CS	cold storage
DNW	distribution network
ECP	extended cutting plane method
el	electrical
ERC	Energy Research Center
EV	evaporator
GHG	greenhouse gas
GTF	geothermal field
gen	generated
HP	heat pump
HPS	heat-pump-system

Continued on the next page

Indices and Abbreviations

Symbol	Meaning
HS	heat storage
HTS	high-temperature-system
HVAC	heating, ventilation, and air conditioning
HX	heat exchanger
HXS	heat-exchanger-system
L-BFGS-B	limited-memory Broyden-Fletcher-Goldfarb-Shanno algorithm with bound constraints
MPC	model predictive control
opt	optimal
PID	proportional-integral-derivative
PSO	particle swarm optimization
rh	relative humidity
RMSE	root-mean-square error
RPE	reduction of performance of the employees
SLSQP	sequential quadratic programming

List of Figures

List of Tables

1 Introduction

The objective of the European Union is to decrease the annual greenhouse gas (GHG) emissions by 80 to 95 percent in 2050, compared to 1990. Moreover, interim targets are set for 2020 and 2030, in which the emissions should decrease by 20 % and 30 %, respectively. Furthermore, the international community agreed on the goal of a GHG neutral global economy between 2050 and 2100. Additionally, an increase in renewable energies and a reduction of primary energy consumption should be introduced [BMU, 2020]. The effects of climate change can already be seen. Among others, the melting of the ice causes significant sea-level rise [Ankel, 2020].
GHG emissions are mainly caused by energy consumption. In Germany, approximately 40 % of energy consumption is caused by buildings. Therefore, the 18 million residual buildings and the 1,5 million non-residual buildings show great potential for decreasing the total energy consumption [BMWI, 2020].

Many studies have been done to decrease energy consumption in the building sector. The energy system of the majority of buildings is regulated by classical controllers. The category of classical control strategies contains e.g. the PID-controller or on/off controllers. However, it has been shown, that more complex control mechanisms can ensure a decrease in energy consumption and a reduction of the energy costs [Lanz, 2019]. One of the more advanced strategies is the model predictive control (MPC). Nevertheless, MPC increases modeling effort and computational complexity. Therefore, distributed model predictive control strategies are increasingly being considered. In distributed approaches, the system is divided into several subsystems. Each subsystem is controlled by an agent. Therefore, the system is called a multi-agent-system. Kümpel et al. propose an agent-based control strategy with the presence of a coordinating agent, which supervises the activities of the agents. Due to the presence of the coordinator, this approach is identified as a hierarchical multi-agent-system.
This thesis introduces a hierarchical multi-agent-system to initiate an operational optimization for building energy systems.

Figure 1.1 shows the structure of this work. First, the basics of optimization are described. Besides the mathematical foundations of optimization and the classification of different optimization methods, the optimization algorithm implemented in this thesis is described more precisely. Furthermore, control strategies and, especially, the model predictive control is explained. The state of the art is completed by a section on multi-agent-systems and their related work.

The operational optimization is applied to the energy system of the main building of the E.ON Energy Research Center. After explaining the components of the application system, the development of the multi-agent-system is explained. Furthermore, a visualization of the implementation structure is given.

The operational optimization is validated in a simulation. After the attained results are analyzed, the thesis is closed by a summary and an outlook.

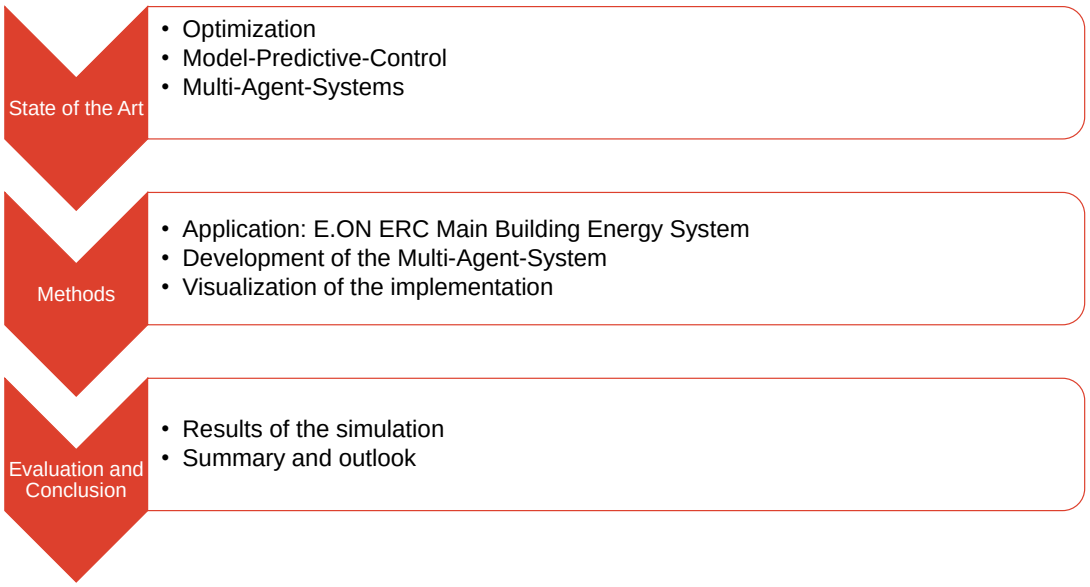

Figure 1.1: Structure of this work

2 State of the Art

2.1 Building Energy Systems

Buildings make up for a huge percentage of the consumed energy and the resulting carbon emissions. Due to the increase of the world's population, the energy consumption in buildings has significantly increased in the past years. Consequently, models, controls, and simulations of buildings are developed, that aim at reducing these negative factors. These improvements would lead to a more sustainable operation [Harish and Kumar, 2016].

Building energy systems are defined as the systems, which cause energy consumption within buildings. They operate to ensure specific conditions, e.g. given by the occupants, to influence their behavior and comfort. Those demands are usually fulfilled with the usage of heating, ventilation, and air-conditioning (HVAC) systems.

HVAC systems consume about 40-60 % of the total energy in buildings [Harish and Kumar, 2016]. Therefore, building energy systems and especially HVAC systems need to be optimized to exploit their fullest and most sustainable potential. Optimization, in general, has become an important field of research for engineers, especially related to the energy sector [Dincer et al., 2017].

When dealing with building energy systems, one of the main optimization approaches is defining the temperature, which is set for the occupants. An increase of this temperature introduces the usage of heating components, such as boilers, heat pumps, heat exchangers, heat storages, or combined heat and powers. The operation of those components can be optimized and controlled. For instance, the output temperature or the mass flow of the components can be determined through an optimization process. The optimization variables specify the needed input energy of the components. Also, the specification of e.g. the mass flows defines the setting of the valves. Altogether, it is crucial to consider the interaction of the building energy system's components, to guarantee a cohesive operational optimization.

2.2 Optimization

Optimization problems are one of the most profoundly researched topics in the field of mathematics. Its applications are versatile, ranging from business to the engineering section [Yang,

2010]. Many engineering problems aim at increasing a specific cost-benefit ratio. This improvement implies a reduction, or more specifically, a minimization of the considered costs to ensure an optimized solution of the problem [Yang, 2010]. The basics of general optimization are indispensable to understand and solve problems occurring in the field of control engineering.

$$f^0 \coloneqq \min_u \{f(u) | u \in U\} \tag{2.1}$$

Equation 2.1, mentioned in the work of Rawlings et al., shows the definition of the value f^0, which is the minimum of the function f. The input variable of the function is u, which is defined in the set U. If the determined value f^0 can be accessed through evaluating f at a point $u \in U$, f^0 is called the minimum. If f^0 lays outside of the image region, it is called the infimum.

$$u^0 \coloneqq arg\,\min_u \{f(u) | u \in U\} \tag{2.2}$$

The mathematical statement in equation 2.2 defines the input variable u^0, which minimizes the function in the predefined area. If the evaluation $f(u^0)$ is smaller than any other function value obtained in $u \in U$, u^0 is defined as the global minimization point. Otherwise, u^0 is only locally minimizing the function.
Furthermore, many optimization problems require the minimization of an objective function, while simultaneously meeting other specifications. These specifications are usually formulated as bounds for the input variables and as constraining functions. It exists a distinction between hard and soft constraints; hard constraints have to be satisfied while minimizing the objective function, whereas the violation of soft constraints only increases the costs of the objective function.
Rawlings et al. distinguish optimization problems into convex and nonconvex ones. In general, the local minimum is the smallest value of the function $f(u)$ for a sufficiently small sub-range of the definition area, while the global minimum is smaller than any other value obtained in the considered range. Only when dealing with convex problems, the local minimum can be equated with the global minimum. Therefore, when dealing with nonconvex problems, the global minimum has to be found, to determine the smallest value of the definition area.

Depending on the type of minimum, different optimization algorithms need to be used. Figure 2.1 shows optimization techniques split into local and global ones [Lin et al., 2012]. Whereas global optimization algorithms can exploit local minimization points, local optimization methods cannot find the global minimum. Although global optimization techniques can be used for local optimization problems, the increasing computational complexity when dealing with

global optimizers would lead to decreased efficiency. Hence, optimization algorithms have to be chosen carefully to enable a satisfactory solution of the considered problem.
Many optimization problems, especially in the field of control engineering, are characterized by complexly constrained and nonconvex behavior of the describing functions. As mentioned before, to obtain the global minimum of such problems, a global optimization method has to be utilized.
Furthermore, figure 2.1 distinguishes global optimization methods into deterministic, stochastic, and evolutionary ones. The stochastic optimization algorithm basin-hopping (BH) is described in more detail in section 2.2.1.

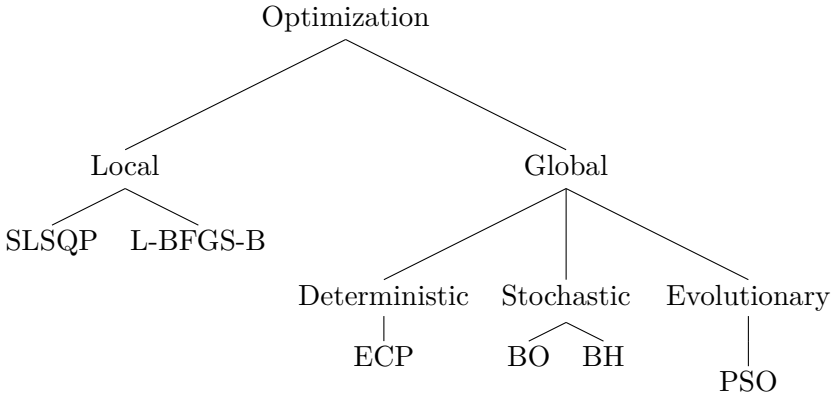

Figure 2.1: Different optimization methods divided into local and global ones. The global optimization techniques include three main types: deterministic, stochastic, and evolutionary.
Abbreviations: sequential quadratic programming (SLSQP), limited-memory Broyden-Fletcher-Goldfarb-Shanno algorithm with bound constraints (L-BFGS-B), Bayesian optimization (BO), basin-hopping algorithm (BH), extended cutting plane method (ECP), particle swarm optimization (PSO)

2.2.1 Basin-Hopping

The basin-hopping algorithm is a global optimizer. It can solve nonlinear and, therefore, hard optimization problems. In particular, basin-hopping is suited to optimize the molecular structure of e.g. proteins. Apart from being able to find the global minimum of the function, the algorithm can also return the other identified local minima. In addition, it has the ability to deal with multiple input variables [Olson et al., 2012].

Abstracted, the algorithm is a combination of global stepping with local minimization, which goes through the following three steps:

1. Input variables are randomly perturbed
2. Local minimization process
3. New input variables are accepted or rejected

After the input variables are chosen, the local optimization in the surrounding of those variables is done. The process of local optimization in the basin-hopping algorithm leads to a transformation of the function $f(\mathbf{u})$, which can be seen in equation 2.3 [Wales and Doye, 1997].

$$\widetilde{f}(\mathbf{u}) = min\{f(\mathbf{u})\} \tag{2.3}$$

This conversion changes the objective function ($f(\mathbf{u})$) into horizontal lines ($\widetilde{f}(\mathbf{u})$). Those horizontal lines, shown in figure 2.2 are also called plateaus or basins. The basins represent the local minima of each considered sub-range (cf. fig. 2.2). The smallest function value $f(\mathbf{u^0})$ obtained by the basin-hopping algorithms, is equivalent to the value of the smallest horizontal line $\widetilde{f}(\mathbf{u^0})$.

During the third step of the optimizing method, the basin-hopping optimization algorithm needs to decide, whether or not to accept the function evaluation. The new function evaluation would serve as an added local minimum, which would then be shown as an added horizontal line in figure 2.2. The basin-hopping algorithm accepts steps in which $f(\mathbf{u}_{new})$ is smaller than $f(\mathbf{u}_{old})$. This simplified approach is called the monotonic basin-hopping method. If, in addition, other steps should be accepted as well, a temperature parameter T_{met} unequal to zero has to be introduced. T_{met} is used in the Metropolis criterion 2.4, to decide about the acceptance of the function evaluation. The temperature parameter determines the probability of acceptance P_{met}. If the calculated probability is greater than a predefined threshold, the function value will be accepted by the algorithm [Sci, 2020].

$$P_{met} = e^{\frac{f(\mathbf{u}_{old}) - f(\mathbf{u}_{new})}{T_{met}}} \tag{2.4}$$

Along with deciding on the acceptance or the rejection of a function evaluation during the third step of the basin-hopping algorithm, the main stochastic element comes to play when perturbing the coordinates. The exploration around the current minimizing point has to be big enough to move out of the local minimum. It is equally important, that the perturbation step is not too huge so that no possible global minimum is skipped [Olson et al., 2012].

SciPy [1] offers a ready-to-use framework of the basin-hopping algorithm, which simplifies the application in Python. An advantage of the basin-hopping method is, that this algorithm

[1] https://docs.scipy.org/doc/scipy/reference/generated/scipy.optimize.basinhopping.html

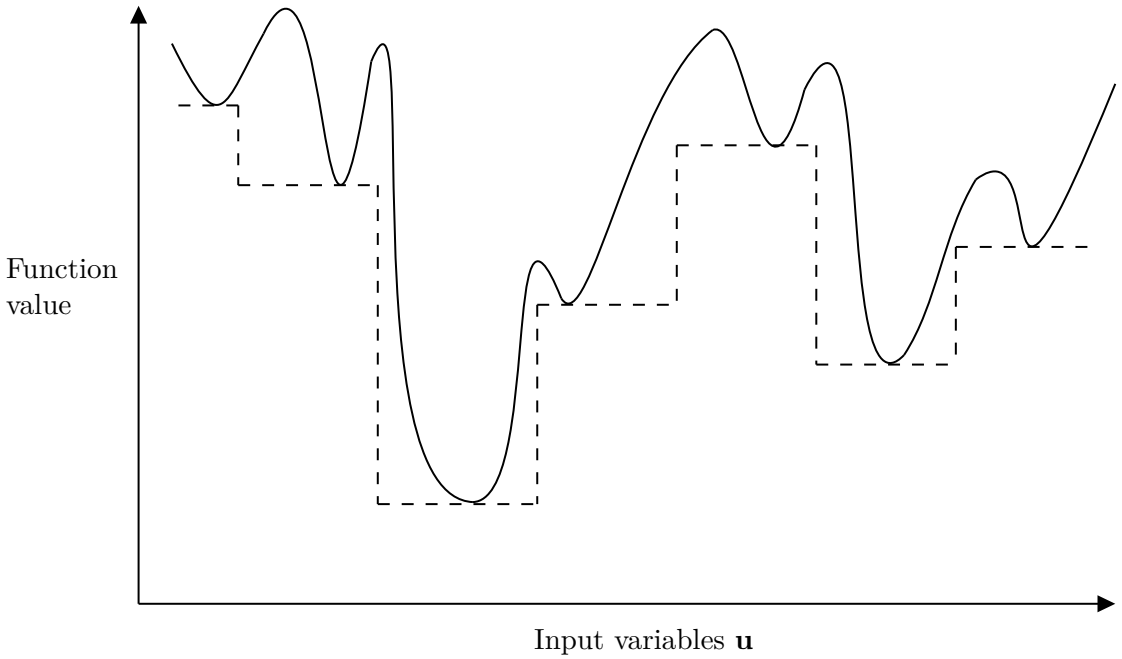

Figure 2.2: The basin-hopping procedure, taken from Wales and Doye [1997].
The solid line represents the objective function $f(\mathbf{u})$, which is being minimized. The horizontal lines are the transformed function $\widetilde{f}(\mathbf{u})$. To find the global minimum of the definition area, the basin-hopping algorithm performs local minimizations. The local minima are transformed into horizontal basins (cf. eq.2.3). The basin-hopping algorithm characterizes the smallest basin as the smallest obtained local minimum. Therefore, it is returned as the global minimum of the problem.

is especially helpful when trying to find the global minimum of composed functions. The minimums of each of the sub-functions, assembling the composed function, usually compete with each other. It is, therefore, harder for an optimizer to find the total minimum of the composite objective function [Olson et al., 2012].
In contrast to the mentioned advantages of basin-hopping, the optimizer always returns the smallest found local minimum as the global one. There is no guarantee, that this function value is the global minimum.

2.3 Model Predicitive Control

The goal of control engineering is to ensure the desired behavior of the controlled system. Many different control mechanisms have been implemented until today. Afram and Janabi-

Sharifi name distinct approaches on how to control a system. In the first place, they differentiate between contrasting types of control. The classical control mechanisms contain e.g. the on/off control and the PID-control. The on/off control is the simplest and the most intuitive way to determine a system's behavior. Regardless, it is unable to control a moving process and it is not sufficiently complex for the vast majority of systems.

Besides the classical control types, there also exists the category of hard control. An example of this category is the model predictive control (MPC), whose principles were first applied in the early 1960s [Ruchika, 2013]. According to Afram and Janabi-Sharifi, MPC is a control mechanism, which can deal with internally or externally caused disturbances. MPC belongs to the category of more advanced controls. Using advanced controls in the section of HVAC systems enables energy savings. Those energy savings are, among others, caused by the ability of the MPC to predict future disturbances, like the ambient temperature [Serale et al., 2018]. To understand the integration of possible future system behavior by the MPC, figure 3.15 is introduced.

In sub-figure 1 of graphic 3.15, the measured current state is circled. From this point, the output of the system can be predicted. Depending on the predicted output, the trajectory of the control variable is determined at the current instant k. Sub-figure 2 shows the current state, the predicted output, and the control variables like the other sub-figure. This graphic, however, shows these values one control time-step later than the other. Whereas sub-figure 1 displays the system's dynamics at the discrete time-step $k = 0$, sub-figure 2 represents the system at $k = 1$.
It is evident, that the predicted output and, therefore, the control variable trajectory changes from one discrete sampling step to another. Because of the shift of the system at every control time-step, this procedure is called the receding horizon.

The predicition horizon (N_p) determines the number of future time-steps the controller considers during the optimization process. The control horizon (N_c) is decisive for the number of future time-steps considered to find the optimal input variables. The bigger N_c is, the more variables have to be optimized in total. Since N_p is always greater or equal to N_c, the input variables from N_c to N_p are set equal to the last optimized input variable, which is determined at the end of the control horizon. The MPC procedure determines the optimal control variables for the control horizon while regarding the whole prediction horizon. The process of optimization is done at every instant k and only the first element of the optimized input array is implemented into the system [Afram and Janabi-Sharifi, 2014].

Countless performance comparisons can be found in research, where the performance of MPC is confronted with other control strategies. In Afram and Janabi-Sharifi's paper, MPC is compared to a PI-controller. The model predictive control strategy outperformed the PI-controller, while concurrently being more robust.

subfigure 1: k = 0

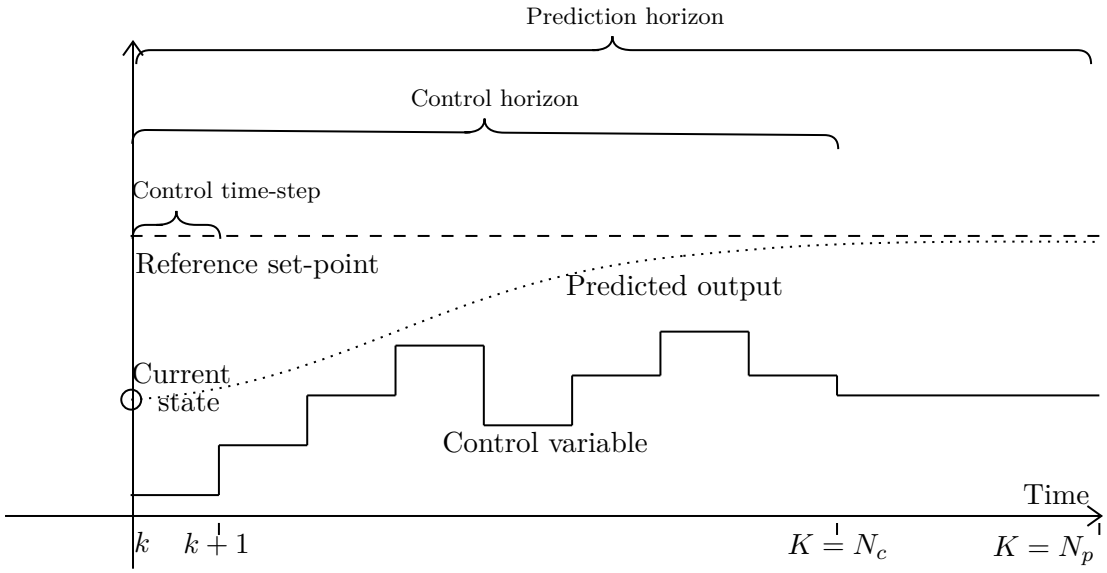

subfigure 2: k = 1

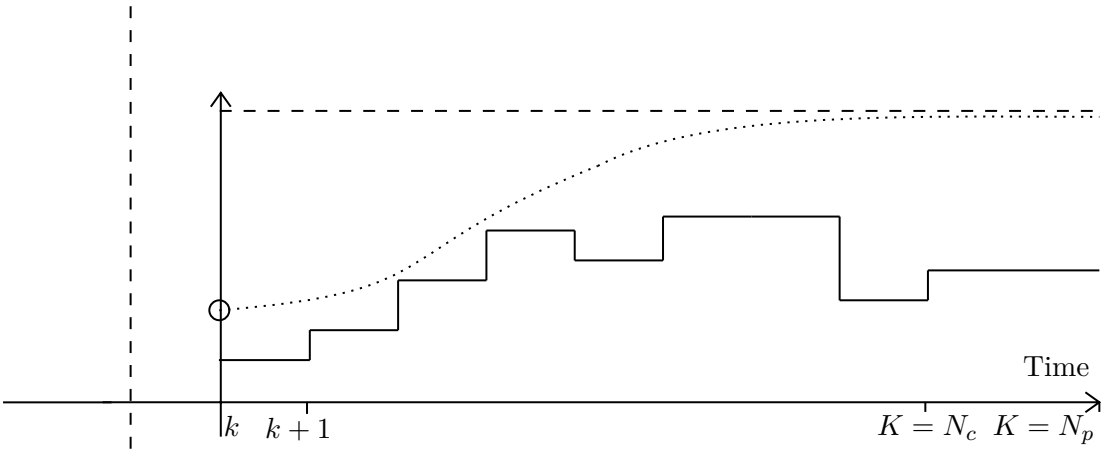

Figure 2.3: Principle of the receding horizon. Sub-figure 2 shows the system's behavior one discrete time-step later than sub-figure 1.

Salem and Mosaad execute a rather thorough comparison between the MPC and the PID-controller. At the start of their paper, they criticize previously performed comparisons published in other papers. The foundation of this criticism results of comparing the MPC to PID-controllers, without optimally tuning the parameters of the classic control approach. Consequently, Salem and Mosaad use the Bacterial Foraging Optimization to optimize the parameters of the PID-controller to ensure a fairer comparison. By studying systems from first to fifth order, they conclude, that in all cases the MPC outperforms the optimized

PID-control in quantitative and qualitative performance indicators.

Another comparison of PID-controllers to model predictive ones is made in the study of Lanz. His results show, that the MPC consumes less heat and electricity than the PID-controller. Additionally, he observes, that the behavior of the MPC can react to changing energy prices. A decrease in the electricity price leads to an increase in the use of electricity to reduce the total costs. This advantage is also mentioned in the work of Afram and Janabi-Sharifi, where the ability to react to changing price structures is a criterion, which has to be fulfilled by an ideal controller.
Besides many measurable advantages of model predictive control, Serale et al. mention an asset of MPC, which cannot be expressed in a quantitative key performance indicator; whenever the circumstances, like the energy prices, change, the parameters can simply be updated. This advantage strongly correlates with the fact, that MPC uses the minimization of a cost function to decide upon its control actions. The general concept of cost functions, as well as the implementation of the cost functions in this thesis, are explained in subsection 2.3.1.

2.3.1 Cost Functions

MPC generates the control vector, which minimizes the cost function (or objective function) over the prediction horizon. In Serale et al., a general approach for cost functions used in model predictive control is given:

$$\begin{aligned} min \sum_{k=1}^{N_p} \Big[W_x \left\| x(k) - x(k)_{set} \right\|_{n_x} + W_y \left\| y(k) - y(k)_{set} \right\|_{n_y} \Big] \\ + \sum_{k=0}^{N_{p-1}} \Big[W_u \left\| u(k) - u(k)_{set} \right\|_{n_u} + W_{\Delta u} \left\| u(k) - u(k-1)_{n_{\Delta u}} \right\| \Big] \end{aligned} \tag{2.5}$$

In equation 2.5, W_i stands for the weight matrices of each component of the cost function, whereas n_i represents the norm, with which each cost vector is transformed into a scalar value. The system states x make up the first part of the cost function. A deviation from the desired set-point is, therefore, penalized. The same principle applies to the output y and input u of the system. In addition, the difference between the implemented input at time-step k and $k-1$ closes the cost function 2.5. The sum of the cost-components is a scalar value to ensure an intuitive and unified comparison with evaluations from different cost functions.

The minimization of a certain cost function enables the implementation of the ideal control step. Nevertheless, before being able to implement an input leading to the desired output, efficient control has to be defined. For this thesis, four criteria are introduced, which characterize an efficient control and operation. The criteria are derived from Spelter [2018].

Spelter, unlike this work, does not want to achieve an operational optimization. Moreover, he compares different control strategies to determine the most efficient one. To measure the quality of the examined control strategies, he introduces four requirements, that the utilization of an ideal controller should lead to:

1. Low energy consumption
2. Satisfactory maintenance of the desired temperature
3. Low CO_2 emissions
4. Low abrasion of the components

The mentioned requirements lead to a cost function consisting of energy costs, thermal costs, CO_2-emission costs and lifetime-reduction costs. The sum, which can be seen in equation 2.6, represents the total cost. The control mechanism that minimizes the total cost is the one, which Spelter characterizes as the best control mechanism.

$$cost = cost_{en} + cost_{th} + cost_{em} + cost_{lr} \tag{2.6}$$

In this work, this approach is taken to determine the most desirable control action and operation. To ensure a thorough insight into cost function 2.6, the elements will be explained.

Energy Costs

Reducing energy consumption and energy costs is one of the main objectives of the optimization of energy systems.
First of all, the required energy has to be determined. For that, an energy balance is needed. The required energy is then divided by the efficiency to calculate the supplied energy.
Care must be taken to ensure that the supplied heat Q_{fuel} or the supplied electricity W_{el} are in units of energy, and not of power. Hence, whenever the result of the energy balance is a heat flow or a power, an integration (cf. eq. 2.7, 2.8) has to be performed. The time-integration ensures a conversion from the required power into the required energy for the time interval δt.

$$Q_{fuel} = \int_{t_0}^{t_0+\delta t} \dot{Q}_{fuel}\ dt \tag{2.7}$$

$$W_{el} = \int_{t_0}^{t_0+\delta t} \dot{W}_{el}\ dt \tag{2.8}$$

Furthermore, the energies are multiplied with the respective costs to determine the energy costs in monetary units (MU). The costs for natural gas, which is needed to generate heat

Parameter	Description	Value
c_{heat}	Price of natural gas	0,06 MU/(kWh)
c_{el}	Price of electricity	0,30 MU/(kWh)

Table 2.1: Parameters for $cost_{en}$

and the electricity costs are taken from average values in Germany (KWH Preis [2020] [2] , STROM-REPORT [2020] [3]). The values are listed in table 2.1. Function 2.9 defines the resulting energy costs used in this thesis.

$$cost_{en} = c_{heat} \cdot Q_{fuel} + c_{el} \cdot W_{el} \tag{2.9}$$

Thermal Costs

The introduction of thermal costs covers the criterion, that a predefined temperature has to be reached inside of a building. The perceived comfort by people in buildings and rooms is characterized by the Mollier-diagram shown, in figure 2.4.

The temperature and the humidity are the variables considered in the visualization of the Mollier-diagram (cf. fig. 2.4). The goal of guaranteeing thermal well-being implies the regulation of the mentioned variables into the illustrated comfort zone.
With this in mind, a deviation from the desired set-point has to introduce a controlled heating, cooling, humidifying, or dehumidifying action to get to the comfort zone. For the sake of simplicity the humidity is not considered in this work. Therefore, the sole focus is on the regulation of the temperature to ensure thermal comfort.

Kümpel et al. penalize a deviation from the set-temperature (cf. eq. 2.10). This is a common approach to control the temperature with the use of a cost function, serving as a soft constraint. Even though function 2.10 is relatively intuitive, its calculated cost cannot be compared uniformly to e.g. energy costs (cf. eq. 2.9).

$$f_{penalty} = (T_{supply} - T_{supply,set})^2 \tag{2.10}$$

Spelter uses a different approach to reach the same goal. With the introduction of a thermal cost function in monetary units, it is possible to quantitatively compare different types of costs. To achieve this business-oriented way of expressing the thermal costs, Spelter calculates the reduction of performance of the employees (RPE) caused by set-temperature deviations. Function 2.11 shows a monetary way of describing thermal costs.

[2] https://www.kwh-preis.de/gas/ratgeber/was-kostet-eine-kilowattstunde-gas
[3] https://strom-report.de/strompreise/strompreisentwicklung/

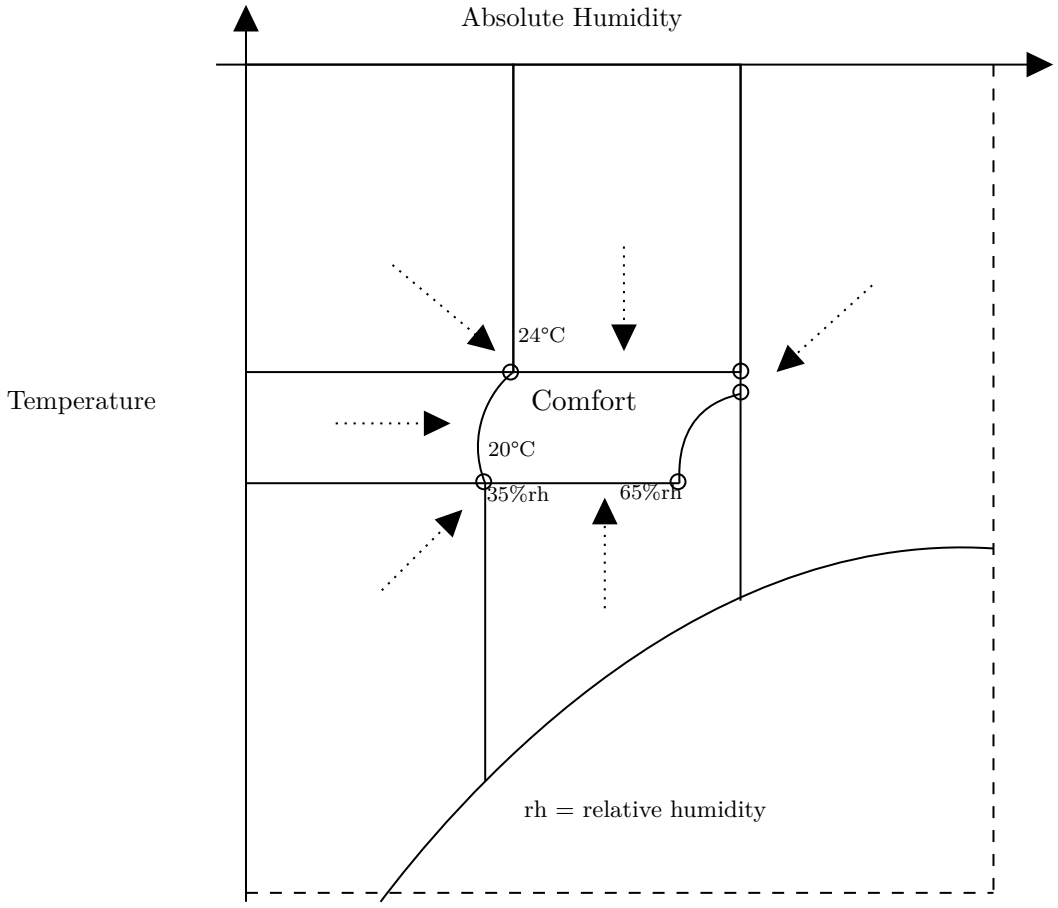

Figure 2.4: Mollier-diagram taken from Müller [2019c].
The objective is to regulate the temperature and the humidity to convert the system's state into the comfort zone.

$$cost_{th} = G \cdot n_p \cdot C_{prod} \cdot \frac{1}{233 \cdot 8 \cdot 60} \cdot \delta t \cdot RPE \tag{2.11}$$

G is the annual income of a person, who is influenced by the thermal conditions present in the considered room or building, whereas n_p defines the number of people affected. The productivity factor C_{prod} transforms the annual income of a person into the annual revenue he generates for his employer. The annual income multiplied by the productivity factor and divided by the minutes an employee works per year results in the revenue generated by the employee per working minute. Another multiplication with the time interval δt and the number of persons n_p brings forth the revenue the room or building is generating for the company in one time interval. The contribution of the parameter RPE enables determining, how many monetary units are lost due to the violation of the thermal comfort in the considered area. The values for the parameters G and C_{prod} are taken from Spelter [2018] and listed in table 2.2.

Parameter	Description	Value
G	Annual income	50.000 MU
C_{prod}	Productivity factor	1,3

Table 2.2: Parameters for $cost_{th}$

To calculate the RPE, first of all,the aberration of the temperature from the set-temperature has to be worked out.

$$\Delta T_{dev} = T - T_{set} \tag{2.12}$$

Second, an allowed deviation δT_{dev} has to be defined. The parameter δT_{dev} defines the temperature difference, in which a deviation from the set-temperature does not cause any thermal costs. Equation 2.13 construes the compilation of the reduction of performance by the employees.

$$RPE(T) = \begin{cases} 0,04 \cdot (\delta T_{dev} - \Delta T_{dev}) & if\ \Delta T_{dev} < -\delta T_{dev} \\ 0 & -\delta T_{dev} \leq \Delta T_{dev} \leq \delta T_{dev} \\ 0,02 \cdot (\Delta T_{dev} - \delta T_{dev}) & if\ \Delta T_{dev} > \delta T_{dev} \end{cases} \tag{2.13}$$

The RPE serves as a relative weighting factor in cost function 2.11. Correspondingly, the parameter can only accept values between zero and one. Function 2.14 clarifies the closure of the RPE parameter.

$$RPE(T) = \begin{cases} 1 & if\ RPE(T) > 1 \\ 0 & if\ RPE(T) < 0 \end{cases} \tag{2.14}$$

It is evident, that if the RPE is equal to zero, the thermal comforting conditions are satisfactorily fulfilled and no thermal costs are generated. A total violation of the thermal comforting conditions is represented by an RPE equal to one. In this case, the highest possible thermal costs are added to the system through function 2.11.

CO_2-Emission Costs

While energy costs and thermal costs are usually considered during the operational optimization of energy systems, direct involvement of the reduction of CO_2-emission costs is rarely seen.
The approach to describe the cost function 2.17 and its parameters are again taken from Spelter [2018]. First, the amount of inputted heat and electricity has to be multiplied with the parameters, which convert the energy into tons of released CO_2.

Parameter	Description	Value
$f_{CO_2,heat}$	Emission-factor heat	0,200 t/(MWh)
$f_{CO_2,el}$	Emission-factor electricity	0,626 t/(MWh)
c_{CO_2}	CO_2-emission cost-factor	19,51 MU/(t)

Table 2.3: Parameters for $cost_{em}$

$$t_{CO_2,Q} = f_{CO_2,heat} \cdot Q_{fuel} \tag{2.15}$$

$$t_{CO_2,W} = f_{CO_2,el} \cdot W_{el} \tag{2.16}$$

Now that the CO_2 mass is calculated, the total amount of tons of released CO_2 is converted into monetary units in function 2.17. The factor transforming the tons of CO_2 into monetary units describes the economic effect of the left carbon footprint.

$$cost_{em} = c_{CO_2} \cdot (t_{CO_2,Q} + t_{CO_2,W}) \tag{2.17}$$

The values of the parameters $f_{CO_2,heat}$, $f_{CO_2,el}$, and c_{CO_2} are visualized in table 2.3.

Lifetime-Reduction Costs

The motivation behind introducing costs, which consider the predicted lifetime of the components is, that with increasing use the abrasion as well increases. The consequence of increasing abrasion is often a decreasing lifetime-expectancy.

An expected lifespan of multi-turn-actuators can be set equivalent to the parameter $T_{10,d}$. The numerical value $T_{10,d}$ is defined as the time, where 63 % of the tested items malfunction. For components, which are used throughout the whole year, $T_{10,d}$ can be calculated with function 2.18.

$$T_{10,d} = \frac{t_{cycle} \cdot B_{10,d}}{365\frac{d}{year} \cdot 24\frac{h}{d} \cdot 3.600\frac{s}{h}} \tag{2.18}$$

The expected cycles in the lifespan of an actuator, $B_{10,d}$, is set to 60.000 [Belimo, 2020].
In addition to the insertion of the parameter $B_{10,d}$, the required time per cycle needs to be quantified. Spelter makes the assumption, that it would take three hours for the actuator to run through a cycle. The mentioned parameters are transmitted into equation 2.19.

Parameter	Description	Value
c_{MTA}	Price of one multi-turn-actuator	200 MU
n_{MTA}	Number of multi-turn-actuators per component	5

Table 2.4: Parameters for $cost_{lr}$

$$T_{10,d} = \frac{10.800\frac{s}{cycle} \cdot 60.000\,cycles}{365\frac{d}{year} \cdot 24\frac{h}{d} \cdot 3.600\frac{s}{h}} = 20,55\ years \tag{2.19}$$

The goal of the introduced lifetime-reduction costs is, that an action, which reduces the expected lifespan of 20,55 years is penalized. While investigating equation 2.18 it becomes obvious, that t_{cycle} is proportional to the expected lifetime. Therefore, a t_{cycle} smaller than the three hours introduced by Spelter, leads to a $T_{10,d}$ smaller than the calculated 20,55 years, and should be penalized.

Equation 2.20 quantifies the lifetime-reduction costs. The parameter c_{MTA} defines the cost of buying a new multi-turn-actuator, whereas n_{MTA} is the number of multi-turn-actuators present in the considered system. This cost is then divided by the number of seconds the component is used per year and multiplied by the time interval δt. Since the costs are scaled by seconds, δt and t_{cycle} also have to be displayed in seconds. The scaling of costs enables the evaluation of the caused costs per regarded time interval.
The scaled acquisition costs are finally multiplied with a weighting factor, which increases, as the abrasion supporting decrease of the parameter t_{cycle} occurs. Furthermore, lifetime-reduction costs only occur, when t_{cycle} is smaller than the predefined three hours by Spelter.

It is assumed, that the system's set-variables change at every time-interval δt. Therefore, a component's cycle is executed within this time-interval. For this reason, t_{cycle} is set equal to δt and the lifetime-reduction costs in 2.20 only depend on the time interval.

$$cost_{lr} = \begin{cases} \frac{n_{MTA} \cdot c_{MTA}}{365\frac{d}{year} \cdot 24\frac{h}{d} \cdot 3.600\frac{s}{h}} \cdot \delta t \cdot \left(1 - \frac{\delta t}{10.800\frac{s}{cycle}}\right) & if\ \delta t < 10.800\frac{s}{cycle} \\ 0 & if\ \delta t \geq 10.800\frac{s}{cycle} \end{cases} \tag{2.20}$$

The value for the cost per multi-turn-actuator c_{MTA} is obtained from APS Arosio GmbH [2020]. To enable a simplified approach, the number of multi-turn-actuators n_{MTA} is regarded as a constant parameter and set to five for every component. The implemented parameters are listed in table 2.4.

2.4 Multi-Agent-Systems

Model predictive control is a rather complex control strategy. Complex control algorithms can lead to negative features when implemented in a centralized way. When handled centrally, the computing time and the computational complexity can be unmanageable [Morosan et al., 2011]. Thereupon, the global problem should be divided into sub-problems. Furthermore, splitting the global problem into sub-problems can simplify the modeling effort of larger systems [Huber, 2016].

With these facts in mind, agent-based implementations or multi-agent-systems are a suited option. Multi-agent-systems follow the approach of solving the global problem by splitting it into several sub-problems. These smaller problems are solved locally by agents [Barbati et al., 2012]. González-Briones et al. characterize an agent as a computer system, which acts autonomously inside a system. Besides the character trait of automation, agents are independent and can communicate [Barbati et al., 2012].

In 2012, most multi-agent-approaches were in the field of scheduling, transport, and logistics. In contrast to these topics, only one agent-based application was used in the energy industry [Barbati et al., 2012].

Barbati et al. point out distributed and centralized agent-based models as the two main approaches of multi-agent-systems. In distributed models, the agents pursue their own goals and organize themselves. Henceforth, they act self-oriented. In contrast, centralized approaches contain a mediator or coordinator agent, which regulates the agents' behavior. The purpose of the coordinator is to find the optimum of the global system. Consequently, a centralized approach is more suitable for global optimizations, because advice can be given from the coordinator to the sub-agents. The coordinator has an abstracted overview of the entire system, whereas the sub-agents only exist in the environment of their respective subsystem. Furthermore, the authors mention, that the implementation of a coordinator could also lead to increased robustness within the system.

2.4.1 Related Work

A multi-agent-system without the usage of a coordinator is given in Elliott and Rasmussen [2012]. The authors develop a system based on neighbor communication between the agents to implement a distributed MPC control. This distributed approach reaches the same global optimum as a centralized MPC.

Huberman and Clearwater employ a centralized multi-agent-system, where agents communicate and negotiate with each other. Since the negotiation of the agents reminds of an auction, the multi-agent-system is an auction-based approach. For this approach, a central

auction-agent is implemented. The auction-agent decides upon the set-points of the sub-agents. Nevertheless, the authors emphasize, that the usage of an omniscient coordinator instead of an auction-agent would enhance the system.

Kümpel et al. present a centralized multi-agent system with the presence of a coordinator applied to an energy system. Since the coordinating agent has an extended decision-making capability in comparison to the sub-agents, these types of implementations are called hierarchical multi-agent-systems. The authors' reason to use this kind of system is to reduce the iterations and the communication effort between the sub-agents. As a result, the sub-agents only communicate with the coordinator and not with each other. The goal of Kümpel et al. [2019] is to reduce energy consumption, while simultaneously keeping a predefined temperature to initiate a small control deviation. To achieve these intentions, the sub-agents create a cost function for their subsystems and hand them over to the coordinator. The coordinator minimizes the sum of the cost functions and returns the set-points for each sub-agent. The determination of the set-points is done with the usage of model predictive control, whereas the set-points inside of the subsystems are set using a PID-controller.

The approach of Lanz is similar to the one of Kümpel et al.. Lanz implements a heat pump, a CHP, a boiler, and a room. These subsystems are controlled by agents. The coordinator determines the set-points for each subsystem after minimizing the cost functions of the sub-agents. Just like in the paper of Kümpel et al., Lanz determines the cost functions through simulation. First of all, the system is simulated. Then, the costs are calculated. Furthermore, these discrete cost-points are transformed into a function through curve-fitting. These fitted functions represent the cost function of each subsystem. The accumulated cost function is minimized by the coordinator through a grid-searching algorithm.

The mentioned applications point out some missing extensions to enhance hierarchical agent-based energy systems. In particular, a consideration of a larger energy system than in Lanz [2019] is desirable. Another key point is, that the cost functions should not precede a completed simulation. Taking these facts into account, this work intends to close the gap created by the missing extensions. In the first place, a larger energy system is examined. Furthermore, the cost functions are not determined through simulation, but are predefined, analytical cost functions. These cost functions are derived from the thesis of Spelter (cf. sec. 2.3.1) and enable a quantitative comparison between each optimization objective.

3 Development of an Agent-Based Optimization

A hierarchical multi-agent-system is developed in this thesis to optimize the operation of a building energy system. The building energy system is divided into subsystems. The interaction between the subsystems is supervised by a coordinator. Furthermore, each subsystem is regulated by a sub-coordinator. The components inside the subsystems are controlled by agents.

Figure 3.1 shows the hierarchical multi-agent structure. The agents determine the costs f, which are caused by their activities and hand them over to their sub-coordinator. The sub-coordinator calculates the sum of the costs of all agents in its subspace. Furthermore, the sub-coordinator returns the attained value F to the coordinator. Moreover, the coordinator defines its cost function, which is equal to the sum of the sub-coordinators' costs. It has to be stated, that not every agent belongs to the subspace of a sub-coordinator. For instance, agent p in figure 3.1 sends its attained costs F_p directly to the coordinator.

The coordinator minimizes its cost function to acquire the optimal coupling variables of the subsystems X_i. The number of sub-coordinators n cannot be generalized. Also, sub-coordinators do not necessarily have to be introduced in every hierarchical optimization problem. The costs F_i are equal to the minimum of the sum of the costs f_{ij}. The costs f_{ij} are emerged by the agents, which belong to the control space of sub-coordinator i. An agent has a model of its component to have an understanding of its environment. This insight provides the means for calculating the costs of the agent's control action. The costs are determined through a cost function generating (cfg) unit. Moreover, an agent contains a local controller to manipulate its control variables, e.g. the valve-opening. After the optimization process is completed, the optimal set-points x_{ij} are adjusted in the agent's component through the local controller.

While figure 3.1 describes the structure of the implemented agent-based optimization, flow chart 3.2, and the corresponding table 3.1 are dedicated to the optimization algorithm. The activity diagram is divided into three swim-lanes. Each swim-lane represents a hierarchical level of the agent-based system. First of all, a simplified cost function is transferred from the agent to the sub-coordinator (1) and from the sub-coordinator to the coordinator (2).

As stated in figure 3.1, the coordinator requires the costs F_i by all sub-coordinators to minimize its cost function. To determine F_i, the sub-coordinators have to minimize the sum of their agents' costs f_{ij}. Therefore, each sub-coordinator has to perform an optimization

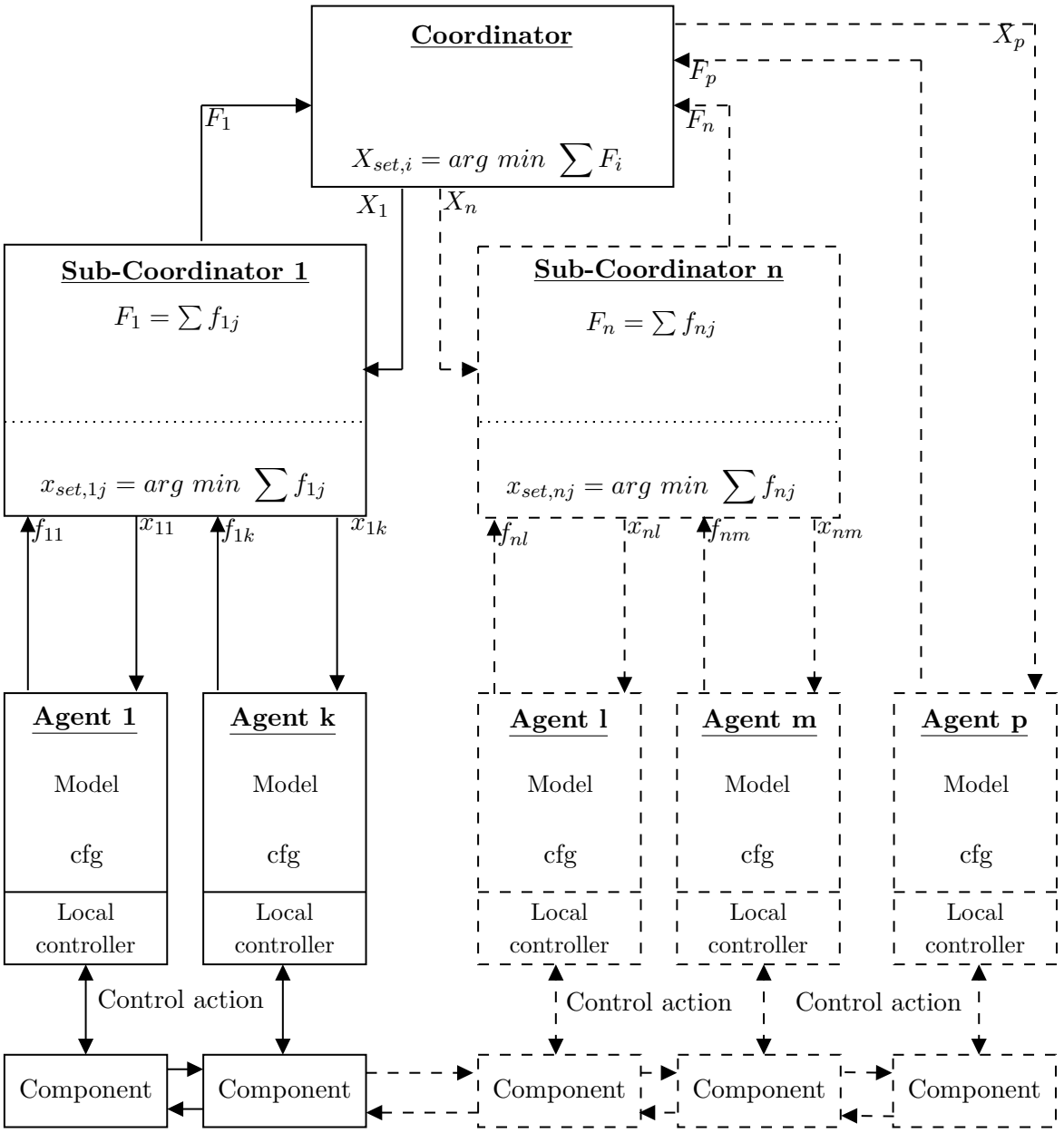

Figure 3.1: Structure of the hierarchical multi-agent-system, derived from [Kümpel et al., 2019]
The coordinator minimizes the sum of the costs given from the sub-coordinators. The sub-coordinators minimize the sum of the costs given by the agents in its subspace. The agents implement the optimal set-variables in their respective component through a local controller.

Node	Affiliation	Activity
(1)	Agent	Hand over the simplified cost function to the sub-coordinator
(2)	Sub-Coordinator	Hand over the simplified cost function to the coordinator
(3)	Coordinator	Start the minimization process with the simplified cost function
(I)	Coordinator	Decision branch
(4)	Coordinator	Specify the coupling variables
(II)	Coordinator	Global minimum or maximum number of iterations reached?
(5)	Coordinator	Hand over the coupling variables to the sub-coordinator
(6)	Sub-Coordinator	Start the minimization process
(III)	Sub-Coordinator	Decision branch
(7)	Sub-Coordinator	Define set-points, that fulfill the coupling variables and hand the set-points to the agents
(8)	Agent	Calculate the value of the cost-creating variable to fulfill the set-points
(9)	Agent	Calculate costs
(10)	Agent	Hand over the costs to the sub-coordinator
(11)	Sub-Coordinator	Determine the sum of all costs given by the agents
(IV)	Sub-Coordinator	Global minimum or maximum number of iterations reached?
(12)	Sub-Coordinator	Hand over the optimal set-points to the coordinator
(13)	Coordinator	Hand over the optimal set-points to control instances

Table 3.1: Description of the activities of the hierarchical algorithm shown in figure 3.2

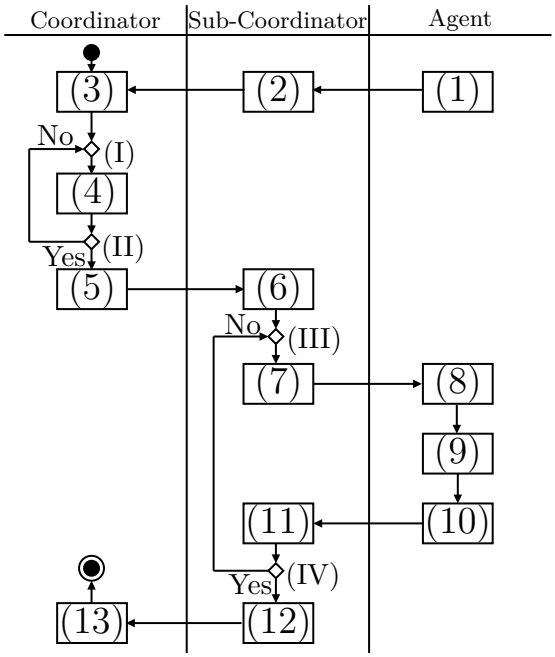

Figure 3.2: Activity diagram of the agent-based optimization algorithm. The hierarchy levels are represented by the individual swim lanes. Table 3.1 describes the activities, which take place at each node.

for every function evaluation of the coordinator's cost function. This would lead to an iterative procedure, where each optimization step of the coordinator requires an accomplished minimization process by the sub-coordinators. This iterative approach results in a nested optimization scheme, which leads to great computational complexity. To avoid this nested and iterative optimization, approximated or simplified cost functions for the sub-coordinators are created in this work.

The coordinator employs the basin-hopping algorithm (cf. sec. 2.2.1) to execute the optimization process (3). The optimization leads to the identification of the optimal coupling variables of the sub-coordinators (4). The sub-coordinators' objective is to fulfill its determined coupling variables with the lowest possible costs. To calculate the variables, which cause minimal costs, the set-variables of the agents have to be specified (6, 7). After defining these variables and handing them over to the agents (7), the agents calculate the costs incurred in meeting the requirements given by its sub-coordinator (8, 9). The cost function, which has to be minimized by the sub-coordinator, consists of the sum of the costs created by each agent in the considered space of the sub-coordinator (10, 11). The global minimum is calculated by the sub-coordinator with the basin-hopping algorithm. If the global minimum or the maximum number of iterations is not reached by the algorithm, the sub-coordinator specifies new set-points for the agents. Otherwise, the optimal set-variables of the agents'

components are transferred to the coordinator (12). The optimal set-points of the agents are defined as the operating point, which causes the least costs and, therefore, initiates an optimal control sequence. Finally, the coordinator transmits these set-points to control instances, which are embedded in the components' agents (13).

To the author's mind, no application of such an agent-based optimization structure with coordinators, sub-coordinators, and agents exists in the field of energy engineering. Therefore, the distinguishing features between each instance are further showcased.

The coordinator has the highest decision-making capability. Therefore, it determines the coupling variables of its subsystems. The control actions within these subsystems have to fulfill the transferred coupling variables by the coordinator. To attain the optimal variables, the coordinator can perform global optimizations.

Just like the coordinator, the sub-coordinator can execute global optimizations. However, the sub-coordinator can only decide on the set-variables within its subsystem; it has to consider its coupling variables, which it receives by the coordinator. Therefore, the sub-coordinator is located at one hierarchy level below the coordinator. The sub-coordinator contains physical models and equations besides its agents. After determining its operation point, the sub-coordinator can return the costs of operation to the coordinator.

Comparatively, the agent can also return costs to a coordinating instance. However, the agent can only manipulate its control variable to reach the predetermined set-variable. Furthermore, the agent adjusts its control variable through a local controller. In comparison to the coordinating instances, the agent has the least decision-making-capability. Nonetheless, the agent contains mass and energy balances, a local controller, and a cost-function-generator. Therefore, it features the most detailed physical modeling.

Furthermore, the distinctions between coordinators, sub-coordinators and agents are summarized in figure 3.3 and table 3.2.

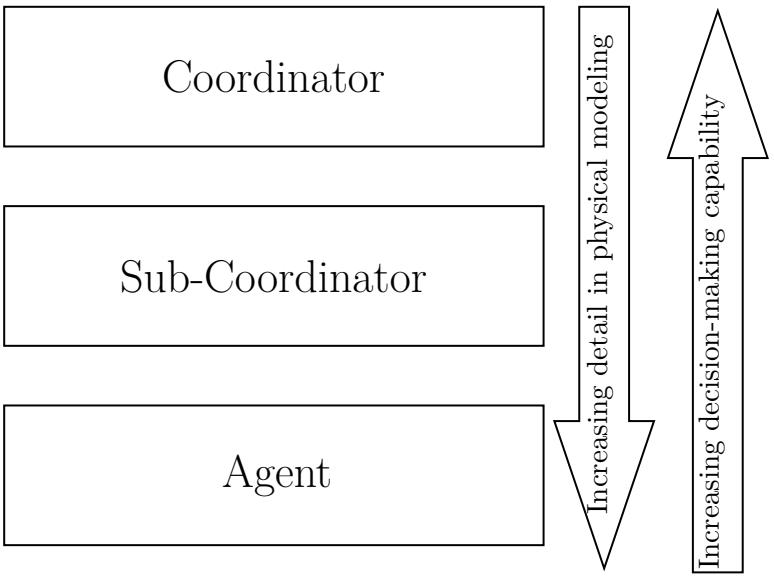

Figure 3.3: The hierarchical order of the coordinator, the sub-coordinator, and the agent. The decision-making capability decreases with descending hierarchy level. In contrast, the level of detail in physical modeling increases from the coordinator to the sub-coordinator, and from the sub-coordinator to the agent.

	Coordinator	Sub-Coordinator	Agent
Overview of the global system	☑	☐	☐
Detailed insight of the subsystem	☐	☑	☐
Execution of a global optimization	☑	☑	☐
Determination of coupling variables	☑	☑	☐
Return of costs	☐	☑	☑
Mass and energy balances	☐	☑	☑
Local controller	☐	☐	☑

Table 3.2: Distinguishing character traits of the coordinator, the sub-coordinator and the agent

3.1 Application of the Agent-Based Structure to the Energy System

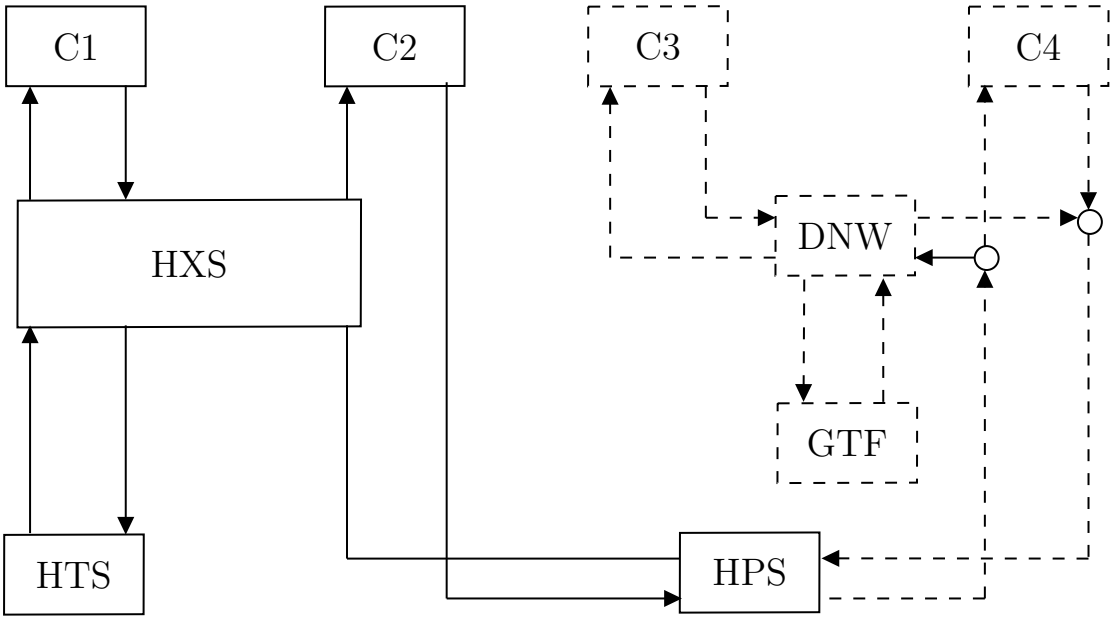

Figure 3.4: Energy system of the E.ON Energy Research Center. The subsystems, which are represented by solid lines are considered during the operational optimization in this work. Abbreviations: C: consumer, HXS: heat-exchanger system, HTS: high-temperature system, HPS: heat-pump-system, DNW: distribution network, GTF: geothermal field

The described agent-based optimization strategy is applied to the main building's energy system of the E.ON Energy Research Center. Figure 3.4 displays a visualization of the mentioned energy system. It contains a high-temperature-system, a heat-exchanger-system, a heat-pump-system, a geothermal field, and a distribution network. Additionally, four consumers are included.

The optimization instance optimizes the operation of the energy system, albeit not every subsystem shown in figure 3.4 is considered during the process of optimization. This work focuses on the application of the agent-based optimization to the high-temperature-system (HTS), the heat-exchanger-system (HXS), and the heat-pump-system (HPS). Furthermore, the first (C1) and the second consumer (C2) are taken into consideration. The HTS contains two boilers and one CHP. The HPS consists of a heat storage, a cold storage, and a heat pump. Moreover, a heat exchanger is the main component of the HXS.

Graphic 3.5 shows the application of the multi-agent structure to the mentioned subsystems. This figure is a simplified and applied display of the previously explained hierarchical multi-agent structure (cf. fig. 3.1). As can be seen, one coordinator regulates the operation of

three sub-coordinators. Each sub-coordinator controls the HTS, the HXS, and the HPS, respectively. In addition to the three sub-coordinators, the coordinator possesses an interface with each of the considered consumers. The consumers do not belong to the subspace of any sub-coordinator.

The sub-coordinator of the HTS regulates the activities of the agent of the first boiler, the agent of the second boiler, and the agent of the CHP. Furthermore, the agent of the heat exchanger is controlled by the sub-coordinator of the HXS. Moreover, the sub-coordinator of the HPS contains the agent of the heat pump in its subspace. As illustrated in figure 3.5, the heat storage and the cold storage are not listed among the agents. Since these components do not contain their own local controller, they are not represented by an agent. Besides the mentioned agents, every subsystem involves a pump-agent. For the sake of simplicity, pump-agents are not illustrated in figure 3.5.

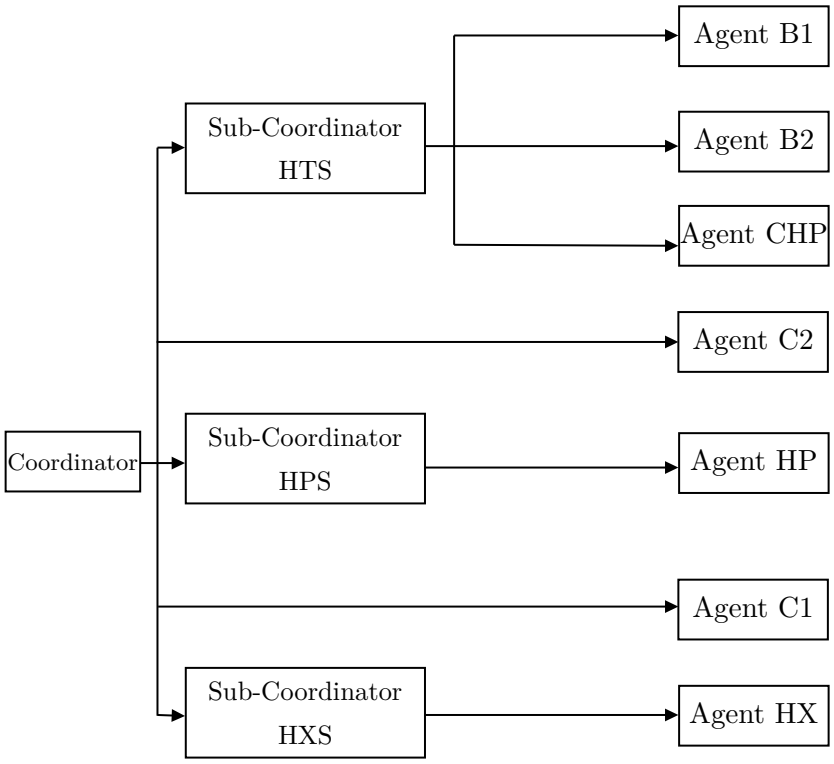

Figure 3.5: Hierarchical agent-based structure applied in this work.
The coordinator is connected to the agents of the consumers and to the sub-coordinators. The sub-coordinators regulate the agents, which are located in their respective environment.

3.1.1 Reference Control

It exists a control strategy to regulate the main building's energy system. This reference control contains predetermined set-points for the energy components and transforms these set-points into control variables. The control variables are determined decentrally. Hence, this control mechanism can also be specified as an agent-based one.

The goal of this work is to enhance the utilized control by a hierarchical multi-agent-system to initiate an operational optimization. In contrast to the reference control, the set-points of the optimized control system are variable. The control instance hands over required parameters to the optimization instance. The agent-based optimization section decides upon the set-variables through a hierarchical multi-agent optimization procedure. Finally, the cost-minimizing set-points overwrite the predetermined ones in the control instance to initiate an optimized operation.

3.2 Agents

In this section, the composition of the agents is explained more precisely. First of all, the relationship between the considered agent and its coordinating instance is described. Subsequently, the model of the agent's component is explained. After examining the environment of each agent, its cost function is presented.

As mentioned in subsection 2.3.1, the costs consist of the penalization of the energy consumption, the CO_2-emission, the temperature deviation of the consumers, and the abrasion of the components. The abrasion-costs exclusively depend on the time interval δt (cf. eq. 2.20). Therefore, changing mass flow or temperature does not affect the lifetime-reduction-costs. Since temperatures and mass flows are optimized within the agent's subspace, the operational optimization does not cause a change in the abrasion-costs. For this reason, $cost_{lr}$ is regarded as a constant. Consequently, $cost_{lr}$ is added to the respective agent. However, the lifetime-reduction costs are not specified any further in this section.

3.2.1 Boiler-Agent

The boiler-agent receives its input and output temperature and its mass flow from the sub-coordinator of the HTS (cf. fig. 3.6). Then, the agent calculates the needed heat flow to reach the output temperature. The required heat flow $\dot{Q}_{fuel,boiler}$ serves as the agent's control variable to reach the controlled variable T_{out}.

$$\dot{Q}_{fuel,boiler} = \frac{1}{\eta_{th,boiler}} \cdot \dot{m} \cdot c_p \cdot (T_{out} - T_{in}) \tag{3.1}$$

The thermal efficiency of the boiler is assumed to be constantly at $\eta_{th,boiler} = 0{,}85$ [Müller, 2019b]. The boiler is modeled with a $\dot{Q}_{fuel,boiler,max}$ of 120 kW.

As explained in subsection 2.3.1, the input heat flow is transformed into the amount of required fuel $Q_{fuel,boiler}$ to increase the temperature in the considered time interval (cf. eq. 2.7). Furthermore, the energy and the CO_2-emission costs are calculated by the boiler-agent. As a result, cost function 3.2 is established and the costs are handed over to the sub-coordinator of the HTS.

$$cost_{boiler} = Q_{fuel,boiler} \cdot (f_{CO_2,heat} \cdot c_{CO_2} + c_{heat}) + cost_{lr} \tag{3.2}$$

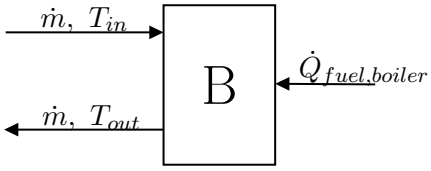

Figure 3.6: Modeling of the boiler-agent: mass flow, input and output temperature, and required heat flow. The agent can determine the heat flow to reach the output temperature.

3.2.2 CHP-Agent

Just as the boiler-agent, the agent of the CHP (cf. fig. 3.7) belongs to the control area of the HTS sub-coordinator. The required $\dot{Q}_{fuel,CHP}$ is calculated identically to equation 3.1. Similarly to the boiler, the control variable $\dot{Q}_{fuel,CHP}$ is needed to reach the output temperature, which is determined by the agent's sub-coordinator. The output temperature serves as the controlled variable of the CHP-agent. In contrast to the boiler, the constant thermal efficiency of the CHP is set to $\eta_{th,CHP} = 0{,}6$ [Müller, 2019a]. Furthermore, the limiting operation point $\dot{Q}_{fuel,CHP,max}$ amounts to 40 kW.

In addition to the obtained output heat flow to increase the temperature of the mass flow, $\dot{Q}_{fuel,CHP}$ generates an electrical power $\dot{W}_{gen,CHP}$ (cf. eq. 3.3). The electrical efficiency $\eta_{el,CHP}$ is set to 25 % (Asue [2020] [1], Müller [2019a]).

$$\dot{W}_{gen,CHP} = \dot{Q}_{fuel,CHP} \cdot \eta_{el,CHP} \tag{3.3}$$

Despite the lower thermal efficiency of the CHP when compared to the boiler, the production of electrical power ensures a higher exergy efficiency. The increased exergy efficiency is

[1] https://asue.de/blockheizkraftwerke

recognized by the agent when calculating the costs. Besides the introduced penalty for lifetime-reduction, emissions, and energy consumption, the cost function of the CHP-agent contains the benefit factor $b_{el,CHP}$.

$$cost_{CHP} = Q_{fuel,CHP} \cdot (f_{CO_2,heat} \cdot c_{CO_2} + c_{heat} - b_{el,CHP} \cdot \eta_{el,CHP}) + cost_{lr} \tag{3.4}$$

The cost factor transforming the produced electrical energy into the benefit is determined semi-empirically. One kilowatt-hour of electricity can be sold for 0,12 MU [Märtel, 2020] [2]. Whenever the considered energy system requires electrical power, the production of electricity by the CHP can replace the external purchase of electricity. In this case, the CHP would prevent the purchase of 0,30 MU per kilowatt-hour [STROM-REPORT, 2020] [3]. It is approximated, that 50 % of the generated electricity is sold, while the rest can be integrated within the system itself. Therefore, a benefit-factor of $b_{el,CHP} = 0,21 \frac{MU}{kWh}$ arises. Furthermore, the value of cost function 3.4 is transferred from the CHP-agent to the sub-coordinator of the HTS.

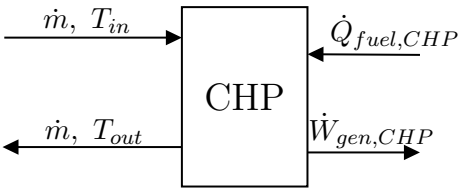

Figure 3.7: Modeling of the CHP-agent: mass flow, input and output temperature, required heat flow, and the resulting generated electricity. The agent can determine the heat flow to reach the output temperature

3.2.3 Heat-Exchanger-Agent

The agent of the heat exchanger is the only one present in the subspace of its organizing sub-coordinator. The sub-coordinator of the HXS hands over the input temperature $T_{cold,in}$ and the mass flow to the agent (cf. fig. 3.8). Furthermore, the sub-coordinator defines the optimal set-temperature $T_{cold,out}$, which is the controlled variable of the agent. The control variable of the agent is the valve-setting. The agent manipulates the setting of the valve autonomously to reach the desired set-temperature $T_{cold,out}$. Moreover, the agent calculates its cost of operation and transmits it to the sub-coordinator of the HXS. Since the desired temperature increase does not require any fuel or electricity input, the agent of the heat-exchanger does not generate any energy or emission costs. Therefore, the only cost transferred from the heat-exchanger-agent to the sub-coordinator is its lifetime-reduction cost.

[2] https://www.solaranlagen-portal.com/solar/lohnt-sich-eine-solaranlage
[3] https://strom-report.de/strompreise/strompreisentwicklung/

$$cost_{HX} = cost_{lr} \tag{3.5}$$

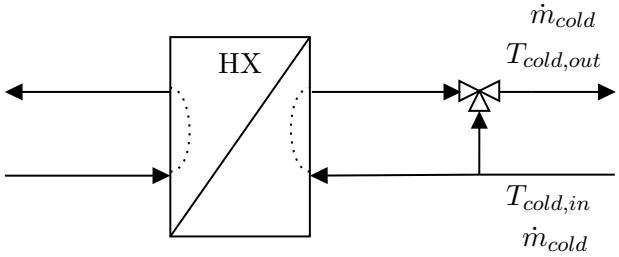

Figure 3.8: Modeling of the heat-exchanger-agent: mass flow and input and output temperature. The agent can determine the valve-setting to reach the desired output temperature.

3.2.4 Heat-Pump-Agent

The heat-pump-agent is located in the control space of the HPS-sub-coordinator. From the sub-coordinator, the agent receives the mass flows $\dot{m}_{CO}$ and $\dot{m}_{EV}$ (cf. fig. 3.9). Furthermore, the input temperatures of the evaporator side and the condenser side are predetermined. The sub-coordinator defines the optimal temperature $T_{CO,out}$ and hands it over to the agent of the heat pump. The output temperature on the condenser side is the controlled variable of the agent. Then, the agent calculates the required heat flow $\dot{Q}_{HP,CO}$ to reach the desired set-temperature.

$$\dot{Q}_{HP,CO} = \dot{m}_{CO} \cdot c_p \cdot (T_{CO,out} - T_{CO,in}) \tag{3.6}$$

The heat-pump generates $\dot{Q}_{HP,CO}$ through the input of an electrical power $\dot{W}_{el,HP}$. The electrical power $\dot{W}_{el,HP}$ acts as the control variable of the heat-pump-agent. This control variable is derived from a division of the heat flow on the condenser side and the coefficient of performance ϵ_{HP} (cf. eq. 3.7). Moreover, the coefficient of performance is set to $\epsilon_{HP} = 6$. The value of this coefficient is obtained through a simulation of the considered energy system.

$$\dot{W}_{el,HP} = \frac{\dot{Q}_{HP,CO}}{\epsilon_{HP}} \tag{3.7}$$

The agent transforms the electrical power into electrical energy $W_{el,HP}$. Furthermore, the agent calculates the cost of operation and returns it to the sub-coordinator.

$$cost_{HP} = W_{el,HP} \cdot (c_{el} + f_{CO_2,el} \cdot c_{CO_2}) + cost_{lr} \tag{3.8}$$

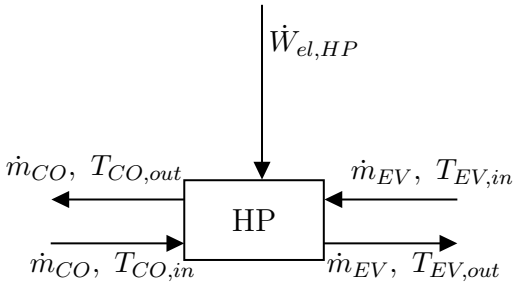

Figure 3.9: Modeling of the heat-pump-agent: mass flow, input and output temperature, and electrical power into the heat pump. The agent can determine the electrical power to reach the output temperature on the condenser side. Abbreviations: CO: condenser, EV: evaporator

In addition to the costs, the agent returns the resulting output temperature of the evaporator side to its sub-coordinator.

$$\dot{Q}_{HP,EV} = \dot{Q}_{HP,CO} - \dot{W}_{el,HP} \tag{3.9}$$

$$T_{EV,out} = T_{EV,in} - \frac{\dot{Q}_{HP,EV}}{\dot{m}_{EV} \cdot c_p} \tag{3.10}$$

Heating up the mass flow in the condenser leads to a decrease in the temperature of the mass, which flows through the evaporator.

3.2.5 Pump-Agent

The control variable of the pump agent is the pump speed. The pump speed is adjusted to handle the volume flow of the pump, which acts as the controlled variable. The operation of the pumps is not optimized by any sub-coordinator. Therefore it is assumed, that the usage of a pump introduces an input power of 0,3 kW. After transforming this power into the required energy for the considered time interval, the agent can determine the costs of operation.

$$cost_{pump} = W_{el,pump} \cdot (c_{el} + f_{CO_2,el} \cdot c_{CO_2}) + cost_{lr} \tag{3.11}$$

Although the pump-agent's set-variable is not optimized by the hierarchical multi-agent-system, it has to manipulate its pump speed to reach the predetermined volume flow. Furthermore, the return of its operational costs influences the cost function of the sub-coordinator.

Since the agent of the pump automatically determines its control variable, it acts independently. The exchange of the agent's operational costs with its sub-coordinator accentuates the ability of communication of the agent. Consequently, the pump-agent fulfills the character traits of an agent. Despite the lack of the explicit involvement of the pumps in the operational optimization, their agent's existence is indispensable.

3.2.6 Consumer-Agent

The coordinator has a direct interface to both considered consumers (cf. fig. 3.4). The set-temperature of the consumer is optimized by the coordinator. In return, the coordinator receives the thermal costs from the consumer-agent. Thermal costs arise when the desired input temperature of the consumer is not met by the coordinator. Furthermore, this temperature deviation leads to a reduction in productivity of the employees. The concept of this cost function has already been introduced in section 2.3.1.

$$cost_{consumer} = G \cdot n_p \cdot C_{prod} \cdot \frac{1}{233 \cdot 8 \cdot 60} \cdot \delta t \cdot RPE \tag{3.12}$$

The consumer-agent manipulates its valve-setting to determine the temperature inside of the consumer's system. Nevertheless, this work does not model the temperature inside of the consumer; it only considers the input temperature. With this simplified approach it is assumed, that with the provisioning of the input temperature, the consumer-agent can control the temperature inside its component. For this reason, this thesis equates the consumer's temperature to its input temperature.

3.3 Sub-Coordinators

After covering the agents, this section dedicates itself to the description of the sub-coordinators. The agent-based optimization scheme contains a sub-coordinator for the HTS, the HXS and the HPS, respectively. Sub-coordinators are located at one hierarchy level above the agents. In contrast to the agents, the sub-coordinators perform global optimizations to define the cost-minimizing operation point of their subsystems. While minimizing the cost of operation, the sub-coordinators have to fulfill the requirements, which are sent by the coordinator. These requirements serve as coupling variables of the sub-coordinator's subsystem.

In mathematical terms, the coupling variables serve as a constraint for the optimization procedure of the sub-coordinator. The global optimization is performed with the basin-hopping algorithm, which has been described in section 2.2.1. The algorithm can handle an optimization with hard or soft constraints. This thesis employs a basin-hopping algorithm

with soft constraints to reach a cost-minimizing operation, while simultaneously meeting the transferred coupling variables. Therefore, the constraints are integrated within the cost function itself. It is a necessary condition, that the solution of every cost function employed in this thesis, converges to the solution of the cost function of the operation if the constraints are met. Therefore, a fulfillment of the constrains precedes the minimization of the operational costs.

3.3.1 High-Temperature-System

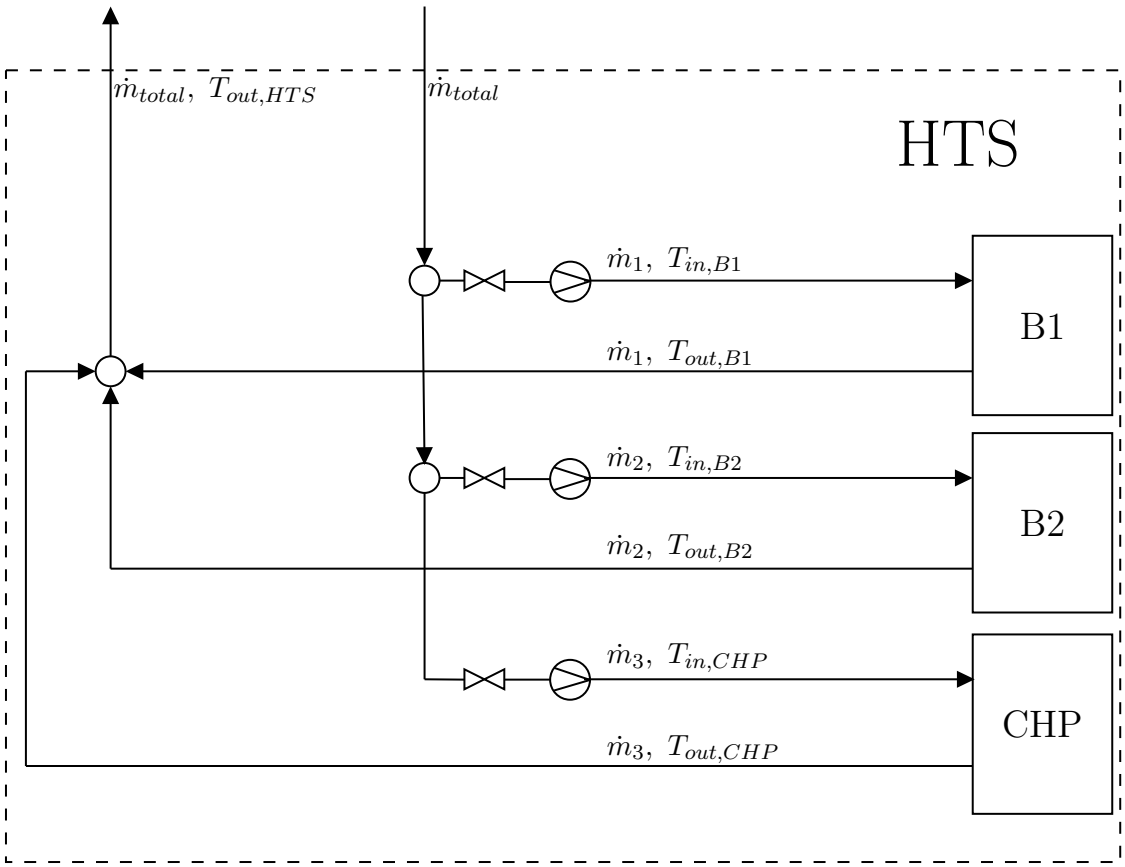

Figure 3.10: Modeling of the sub-coordinator of the HTS: The sub-coordinator's view of the high-temperature-system. The output temperature two boilers and one CHP is optimized to determine the cost-minimizing operation to reach the predetermined output temperature $T_{out,HTS}$.

The objective of the sub-coordinator of the HTS is to minimize the cost of operation of its agents. To achieve this, the sub-coordinator defines the set-temperature of the CHP and both boilers. In return, the sub-coordinator receives the costs of the operation. Furthermore, it has to fulfill the requirements of the coordinator. After minimizing its cost function, the

sub-coordinator transfers the attained costs to the coordinator.

Graphic 3.10 shows the sub-coordinator's view of the high-temperature-system. The sub-coordinator receives the mass flows and the input temperature by the coordinator. Furthermore, the coordinator defines the set-temperature $T_{out,HTS,set}$ of the subsystem. The sub-coordinator aims to reach the set-temperature with minimal costs.

The input temperature can be increased with the usage of the boilers and the CHP. The three components are connected in parallel. The mass flows $\dot{m}_1, \dot{m}_2$, and $\dot{m}_3$ are predetermined. Therefore, the sub-coordinator can only determine the output temperature of the components to reach the desired set-temperature $T_{out,HTS,set}$.

First, the sub-coordinator hands over the mass flows and the input and output temperatures to the agents. Second, the agents calculate the cost of operation and return it to their sub-coordinator. Then, the sub-coordinator can calculate the total cost of operation.

The composed output temperature $T_{out,HTS,act}$ is calculated with the energy balance 3.14.

$$\dot{m}_{total} = \dot{m}_1 + \dot{m}_2 + \dot{m}_3 \tag{3.13}$$

$$T_{out,HTS,act} = \frac{\dot{m}_1 \cdot T_{out,b1} + \dot{m}_2 \cdot T_{out,b2} + \dot{m}_3 \cdot T_{out,CHP}}{\dot{m}_{total}} \tag{3.14}$$

The cost function of the sub-coordinator consists of the addition of the costs determined by the agents of the boilers and the CHP (cf. eq. 3.2, 3.4). Furthermore, the cost of the pumps is considered (cf. 3.11). Three pumps are located inside the high-temperature-system.

$$cost_{pumps} = 3 \cdot cost_{pump} \tag{3.15}$$

$$cost_{operation,HTS} = cost_{b1} + cost_{b2} + cost_{CHP} + cost_{pumps} \tag{3.16}$$

These operational costs need to be minimized, while simultaneously meeting the given output temperature $T_{out,HTS,set}$ by the coordinator. Thus, the sub-coordinator aims to equate $T_{out,HTS,act}$ and $T_{out,HTS,set}$. This requirement is stated in equation 3.17 and serves as a constraint for the optimization problem.

$$cost_{cons,HTS} = |T_{out,HTS,act} - T_{out,HTS,set}| \tag{3.17}$$

As mentioned at the beginning of this section, constraints are integrated within the cost function itself. If the optimization variables $T_{out,b1}, T_{out,b2}$, and $T_{out,CHP}$ fulfill the constraint, the

cost of the constraint equates to zero. The pre-factors a and c and the dimensions b and d of the constraint costs are determined empirically. The numerical values of these parameters are summarized in table A.1 in the appendix. Moreover, it is important to introduce a significant penalization, if the sub-coordinator fails to meet the coordinator's requirements.
Equation 3.18 represents the cost function of the HTS. In essence, the sub-coordinator minimizes function 3.18 and returns the attained cost, the output temperatures of both boilers, the output temperature of the CHP, and the actual output temperature of the HTS to the coordinator.

$$\begin{aligned} cost_{HTS}\left(T_{out,b1}, T_{out,b2}, T_{out,CHP}\right) = \\ a \cdot cost_{cons,HTS}^{b} + c \cdot cost_{cons,HTS}^{d} \cdot cost_{operation,HTS} + cost_{operation,HTS} \end{aligned} \tag{3.18}$$

If the constraints are met by the sub-coordinator, the cost function of the HTS equates to the sum of the operation costs (cf. eq. 3.19). Therefore, the solution of cost function 3.18 converges to the minimum of the operational costs, if the constraints are fulfilled.

$$cost_{HTS}\left(cost_{cons,HTS} = 0\right) = cost_{operation,HTS} \tag{3.19}$$

Approximation of the HTS

As the algorithm in figure 3.2 points out, the sub-coordinator hands over a simplified cost function to the coordinator. In the first place, the coordinator aims to find the optimal coupling variables for the sub-coordinators. Until these coupling variables are determined, an optimization by the sub-coordinators is not necessary; a sole determination of the costs arising from the proposed coupling variables is sufficient. Since the calculation of the exact costs requires an optimization by the sub-coordinator, an approximated approach to determine the costs is introduced.

For the high-temperature-system, the approximated cost function is derived analytically by performing an energy balance. Due to the higher exergy efficiency, the CHP's operation causes fewer costs when compared to the boiler. Therefore, it is assumed, that the sub-coordinator tries to heat the given mass flow with the CHP. If the maximum power of the CHP is exceeded, the sub-coordinator activates the boilers. With the predetermined mass flows and the implemented maximum operation point of the CHP, a temperature increase of up to 1,5 K can be handled by the CHP individually. Additional heat flow has to be obtained by the boilers. Therefore, the approximated cost function is represented by the piecewise linear cost function 3.20.

$$cost_{HTS,approx} = \frac{1}{\eta_{cost}} \cdot c_{heat} \cdot \dot{m}_{total} \cdot c_p \cdot \Delta T \tag{3.20}$$

The cost-factor η_{cost} decreases, if ΔT exceeds 1,5 K.

$$\eta_{cost} = \begin{cases} 4 & if\ \Delta T < 1,5\,K \\ 3 & if\ \Delta T \geq 1,5\,K \end{cases} \tag{3.21}$$

It has to be stated, that equation 3.20 only approximately represents the behavior of the high-temperature-system. These semi-empiric parameters are acquired from an energy balance of the subsystem and are therefore derived from thermodynamic considerations.

3.3.2 Heat-Exchanger-System

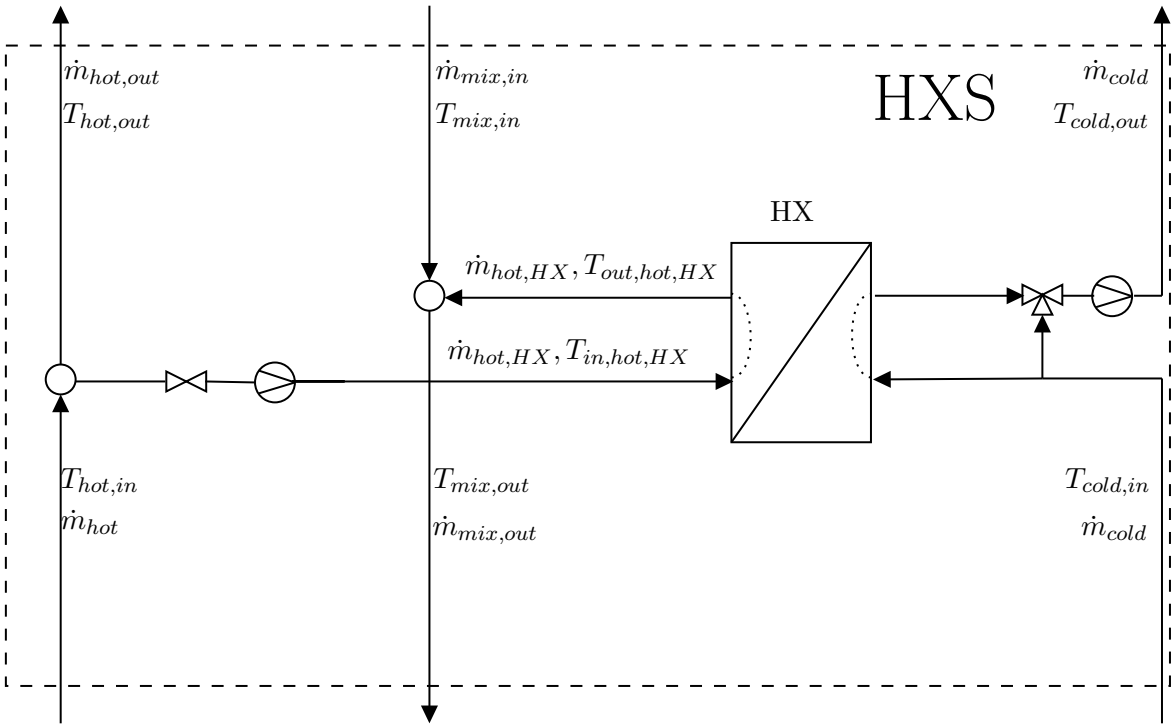

Figure 3.11: Modeling of the sub-coordinator of the HXS: The sub-coordinator's view of the heat-exchanger-system. The mass flow of the hot side of the heat exchanger is optimized to determine the cost-minimizing operation to reach the predetermined output temperature on the cold side $T_{cold,out}$.

The coordinator hands over the mass flows $\dot{m}_{hot}$, $\dot{m}_{mix,in}$, and $\dot{m}_{cold}$ to the sub-coordinator of the HXS (cf. fig. 3.11). Besides to the value of the mass flows, their input temperatures are transferred. Furthermore, the sub-coordinator receives the desired output set-temperature $T_{cold,out,set}$.
The sub-coordinator's objective is to reach the mentioned set-temperature with a cost-minimizing operation. To enable an optimized operation, the sub-coordinator can determine

$\dot{m}_{hot,HX}$, which is the mass flow entering the hot side of the heat exchanger. Moreover, the cost of operation is determined. Then, the sub-coordinator of the HXS calculates the resulting mass flows $\dot{m}_{hot,out}$ and $\dot{m}_{mix,out}$. In addition to the mass flows, the sub-coordinator ascertains the resulting temperature $T_{mix,out}$ and the actual temperature of the set-variable $T_{cold,out,act}$. Finally, the sub-coordinator transmits the costs along with the resulting mass flows and temperatures to the coordinator.

First of all, the required heat flow to increase the temperature on the cold side of the heat exchanger is determined.

$$\dot{Q}_{HX,set} = \dot{m}_{cold} \cdot c_p \cdot (T_{cold,out,set} - T_{cold,in}) \tag{3.22}$$

This heat flow is attained from the enthalpy flow on the hot side of the heat exchanger. With the assumption, that the heat exchanger has no heat losses, the resulting output temperature on the hot side can be calculated with equation 3.23.

$$T_{out,hot,HX,set} = T_{in,hot,HX} - \frac{\dot{Q}_{HX,set}}{\dot{m}_{hot,HX} \cdot c_p} \tag{3.23}$$

Since heat can only be transferred from a higher temperature level to a lower one, the resulting temperature $T_{out,hot,HX}$ has to be smaller than $T_{cold,out,set}$. This thermodynamic constraint has to be verified by the sub-coordinator. If the output temperature on the hot side is greater than the output temperature on the cold side, the heat transfer is physically feasible under the circumstances of an ideal operation. In contrast, if this physical constraint is violated, the heat flow has to be calculated again. In this case, the value of the heat flow is determined by the hot side of the heat exchanger.

$$\dot{Q}_{HX,act} = \begin{cases} \dot{Q}_{HX,set} & if\ T_{out,hot,HX,set} > T_{cold,out,set} \\ \dot{m}_{hot} \cdot c_p \cdot (T_{in,hot,HX,set} - T_{cold,out,set}) & if\ T_{out,hot,HX,set} \leq T_{cold,out,set} \end{cases} \tag{3.24}$$

Furthermore, the temperatures $T_{out,hot,HX,act}$ and $T_{cold,out,act}$ are calculated.

$$T_{out,hot,HX,act} = T_{in,hot,HX} - \frac{\dot{Q}_{HX,act}}{\dot{m}_{hot,HX} \cdot c_p} \tag{3.25}$$

$$T_{cold,out,act} = T_{cold,in} + \frac{\dot{Q}_{HX,act}}{\dot{m}_{cold,HX} \cdot c_p} \tag{3.26}$$

If the initial heat transfer is physically feasible, the actual temperatures are equal to the set-temperatures. On the other hand, a deviation from the set-temperature occurs. Furthermore,

a deviation from $T_{cold,out,set}$ results in a violation of the requirements, which are transmitted by the coordinator. The deviation from the transferred set-temperature causes constraint-costs.

$$cost_{cons,HXS} = |T_{cold,out,act} - T_{cold,out,set}| \tag{3.27}$$

The costs of operation are caused by the heat exchanger and the two pumps, which are located inside the HXS.

$$cost_{pumps} = 2 \cdot cost_{pump} \tag{3.28}$$

$$cost_{operation,HXS} = cost_{pumps} + cost_{HX} \tag{3.29}$$

The penalization function, which is minimized by the sub-coordinator of the HXS, is composed of the costs of operation and the constraint-costs (cf. eq. 3.30). The sub-coordinator manipulates $\dot{m}_{hot,HX}$ to enable a cost-minimizing operation.

$$cost_{HXS}\left(\dot{m}_{hot,HX}\right) = a \cdot cost^{b}_{cons,HXS} + c \cdot cost^{d}_{cons,HXS} \cdot cost_{operation,HXS} + cost_{operation,HXS} \tag{3.30}$$

After determining the costs, the sub-coordinator calculates the resulting mass flows and output temperatures.

$$\dot{m}_{mix,out} = \dot{m}_{hot,HX} + \dot{m}_{mix,in} \tag{3.31}$$

$$\dot{m}_{hot,out} = \dot{m}_{hot,in} - \dot{m}_{hot,HX} \tag{3.32}$$

$$T_{mix,out} = \frac{\dot{m}_{mix,in} \cdot T_{mix,in} + \dot{m}_{hot,HX} \cdot T_{out,hot,HX,act}}{\dot{m}_{mix,out}} \tag{3.33}$$

Alongside the attained cost and the optimization variable $\dot{m}_{hot,HX}$, the resulting values for $\dot{m}_{hot,out}$, $\dot{m}_{mix,out}$, $T_{mix,out}$, and $T_{cold,out,act}$ are transferred to the coordinator.

The sub-coordinator only optimizes one variable. Furthermore, obtaining the solution of cost function 3.30 is computationally manageable. Thus, an approximation of the HXS is not employed.

3.3.3 Heat-Pump-System

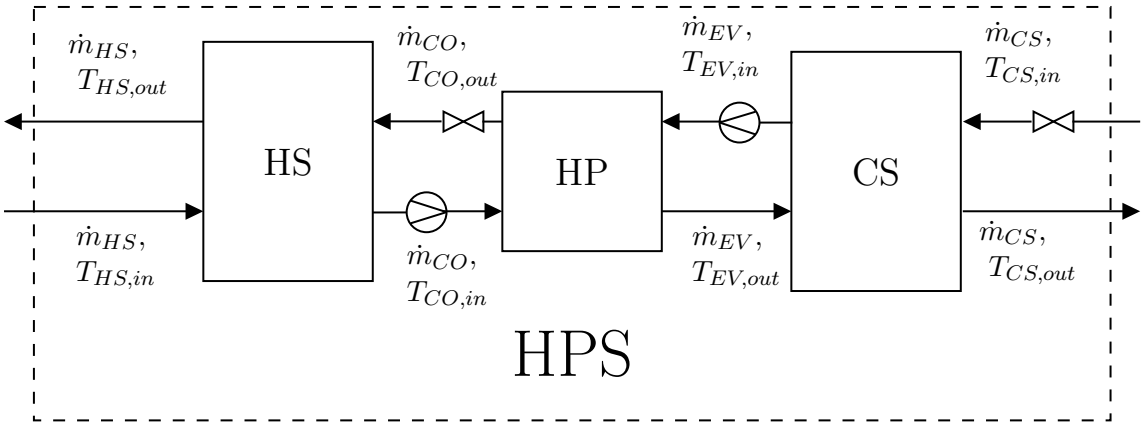

Figure 3.12: Modeling of the sub-coordinator of the HPS: The sub-coordinator's view of the heat-pump-system. The output temperature of the condenser side of the heat pump is optimized to determine the cost-minimizing operation to reach the predetermined output temperature $T_{HS,out}$. The sub-coordinator of the HPS optimizes $T_{CO,out}$ to enable a cost-minimizing operation. Abbreviations: HS: heat storage, CS: cold storage, HP: heat pump, CO: condenser, EV: evaporator.

The sub-coordinator of the heat-pump-system receives $\dot{m}_{HS}$ and its corresponding input temperature from the coordinator. Moreover, the ambient temperature, the initial temperature of the storages, and the mass inflow into the cold storage are defined. Furthermore, the coordinator sends the set-temperature $T_{HS,out,set}$ to the sub-coordinator. Additionally, $\dot{m}_{CO}$ and $\dot{m}_{EV}$ are also predetermined. The sub-coordinator's objective is to minimize the cost of operation, while simultaneously aiming to reach the required temperature $T_{HS,out,set}$.

Figure 3.12 shows the sub-coordinator's insight of its subsystem. Besides the heat pump and its agent, the HPS contains a heat storage and a cold storage. Storages are not represented by agents. Nevertheless, the sub-coordinator has to determine the temperature of the storages. For this reason, the modeling of the storages is derived in the following section.

Modeling of the Storages

To determine the temperature of the storage, a non-stationary energy balance has to be adapted. The derivation of the equation for the internal energy in 3.34 can be found in the appendix (cf. sec. A.2).

$$\frac{dU}{dt} = m \cdot c_v \cdot \frac{dT}{dt} \tag{3.34}$$

Name	Parameter	Value
Density	ρ	1000 kg/(m^3)
Heat capacity (isochor)	c_v	4,2 kJ/(kgK)
Heat capacity (isobar)	c_p	4,18 kJ/(kgK)

Table 3.3: Chemical parameters and their values for water, used while modeling the heat storage and the cold storage

The expression for the time derivate of the internal energy is set equal to the sum of energy flows. Furthermore, the mass of the system is displayed by the multiplication of the volume of the storage and the density of water. Then, the resulting equation is transformed into an explicit expression of the time derivative of the temperature. The mathematical statement in 3.35 represents the ordinary differential equation for the temperature as a function of the time. The temperature profile can be attained by integrating this function.

$$\frac{dT}{dt} = \frac{1}{\rho \cdot V \cdot c_v} \cdot \left[\dot{m} \cdot c_p \left(T_{in} - T\right) - \dot{Q}_{conv}\right] \tag{3.35}$$

Table 3.3 summarizes the chemical parameters, which are used while modeling both storages. The values are taken from Engineering Toolbox [2020] [4] and are treated as constants.

The loss of energy $\dot{Q}_{conv}$ is caused by convective heat flows. The convective heat flow arises from the temperature difference between the storage and the environment.

$$\dot{Q}_{conv} = k \cdot (2 \cdot A_{cover} + A_{shell}) \cdot (T - T_{ambient}) \tag{3.36}$$

Furthermore, the thermal transmittance coefficient k has to be determined. From observations of the simulation of the considered energy system, it can be concluded, that the temperature of the closed storage settles at its stationary operation point after approximately three days. The steady-state is reached if the temperature of the storage is sufficiently close to the ambient temperature. Figures A.1 and A.2 in the appendix show the evaluation of the temperature profiles for $k = 0,02 \frac{\mathrm{kW}}{\mathrm{m^2\,K}}$, respectively.

The starting temperature of the heat storage is set to 305,15 K, whereas the cold storage starts at a temperature of 283,15 K. The ambient temperature amounts to 288,15 K. As can be seen (cf. fig. A.1, A.2), the value of the thermal transmittance coefficient k is chosen reasonably. Therefore, the temperature of the storages settle near the ambient temperature after about three days.

[4] https://www.engineeringtoolbox.com/water-thermal-properties-d_162.html

Name	Parameter	Value
Volume	V	5 m^3
Cover surface	A_{cover}	1,77 m^2
Shell surface	A_{shell}	13,21 m^2

Table 3.4: Values for the volume, the cover surface and the shell surface of the heat storage

Name	Parameter	Value
Volume	V	4 m^3
Cover surface	A_{cover}	1,77 m^2
Shell surface	A_{shell}	10,65 m^2

Table 3.5: Values for the volume, the cover surface and the shell surface of the cold storage

The volume of the cylindrical heat storage is known to be $5\,m^3$. In contrast to the heat storage, the volume of the cold storage amounts to $4\,m^3$. The determined surfaces of the cover and the shell fulfill the geometrical constraints resulting from the determined volume of the storages. Tables 3.4 and 3.5 summarize the geometrical parameters used while modeling the heat storage and the cold storage, respectively.

In essence, the sub-coordinator of the HPS wants to attain the temperature of the storages. The introduced model can determine the temperature profile for the entire time interval. Nonetheless, the sub-coordinator only requires one representative value of the temperature for each time interval. Therefore, the sub-coordinator receives the mean value $\overline{T}$ of the storage temperature by the model.

Alongside the consideration of time, the temperature also depends on the vertical position inside the storage. This dependency can be simplified by only distinguishing between the top and the bottom of a storage.
By evaluating the simulation of the considered energy system, the temperature difference between the upper part and the lower part of the heat storage and the cold storage are approximately ascertained. For the heat storage, a temperature difference of 1,5 K is adopted. In contrast, the difference between the upper and the lower part of the cold storage amounts to 0,1 K. Hence, the temperatures calculated from equation 3.37 to 3.40 are determined by the model of the storage. Furthermore, the representing temperature values are handed over to the sub-coordinator of the HPS.

$$T_{upper,HS} = \overline{T}_{HS} + 0,75\,K \tag{3.37}$$

$$T_{lower,HS} = \overline{T}_{HS} - 0,75\,K \tag{3.38}$$

$$T_{upper,CS} = \overline{T}_{CS} + 0,05\,K \tag{3.39}$$

$$T_{lower,CS} = \overline{T}_{CS} - 0,05\,K \tag{3.40}$$

Cost Determination of the Sub-Coordinator

This work focuses on the optimization of the left part of E.ON ERC's energy system (cf. fig. 3.4). Therefore, the coordinator only determines the set-temperature of the heat storage $T_{HS,out,set}$. The sub-coordinator aims to reach this set-temperature with minimal cost. A deviation from the required output temperature of the heat storage leads to constraint-costs.

$$cost_{cons,1,HPS} = |T_{HS,out,act} - T_{HS,out,set}| \tag{3.41}$$

To reach the set-temperature $T_{HS,out,set}$, the sub-coordinator can determine the temperature of the water exiting the condenser. Increasing the temperature $T_{CO,out}$ requires an input power of the heat pump. The cost value caused by the operation of the heat pump is received by the responsible agent. With knowledge of the coupling variables of the heat storage, the energy balance can be established. Furthermore, the differential equation of the temperature of the heat storage is solved. In return, the sub-coordinator receives the temperature of the upper part of the heat storage (cf. eq. 3.37). This temperature is equal to the temperature $T_{HS,out,act}$, which is the actual temperature exiting the heat-pump-system.
In addition to the heat pump, two pumps are located within the HPS.

$$cost_{pumps} = 2 \cdot cost_{pump} \tag{3.42}$$

The operational cost takes the heat pump and both pumps into consideration.

$$cost_{operation,HPS} = cost_{HP} + cost_{pumps} \tag{3.43}$$

Altogether, equation 3.43 sums up the operational costs of the HPS. Besides fulfilling the requirements by the coordinator, the sub-coordinator aims to minimize these costs of operation.

Through the determination of the optimization variable $T_{CO,out}$ by the sub-coordinator, the temperature $T_{EV,out}$ is specified. The output temperature of the evaporator is returned to the sub-coordinator by the agent of the heat pump. Therefore, every mass flow entering and exiting the cold storage is predetermined. Due to the definiteness of the system, the temperature

of the cold storage cannot be influenced any further by the sub-coordinator. Nonetheless, the temperature of the cold storage should be within a certain temperature interval. Therefore, bounds are introduced for the cold storage. A lower bound is introduced to prevent the water from getting too close to its freezing point. This lower bound is set to 278,15 K. In contrast, an upper bound of 295,15 K guarantees the right side of the energy system reasonably cold water flow. Furthermore, this upper bound assures, that the temperature of the cold storage is lower than the temperature of the heat storage.
The values for the bounds are derived from the simulation of the energy system with the use of the reference control (cf. sec. 3.1.1). Equation 3.44 presents the resulting constraint costs, which arise from a deviation of the cold storage temperature from the predefined temperature interval.

$$cost_{cons,2,HPS} = \begin{cases} 0 & if\ \overline{T}_{CS} > 278,15\,K\ and\ \overline{T}_{CS} < 295,15\,K \\ a & if\ \overline{T}_{CS} \leq 278,15\,K\ or\ \overline{T}_{CS} \geq 295,15\,K \end{cases} \tag{3.44}$$

The sub-coordinator influences the temperature of the cold storage with the determination of its optimization variable $T_{CO,out}$. The introduced penalization for the cold storage solely serves to increase the constraint costs. Moreover, the sum of the constraint costs is determined.

$$cost_{cons,HPS} = cost_{cons,1,HPS} + cost_{cons,2,HPS} \tag{3.45}$$

To calculate the constraint costs, T_{CS} has to be attained by the sub-coordinator. Figure 3.12 displays, that the temperature $T_{EV,in}$ is equal to the temperature of the upper part of the cold storage. The temperature $T_{EV,out}$, which enters the cold storage from the left side, is not an independent variable. Through the determination of the optimization variable $T_{CO,out}$, the output temperature on the evaporator side of the heat pump is a predetermined parameter. Therefore, the temperature of the cold storage is a function of $T_{EV,out}$, which explicitly depends on the temperature of the cold storage itself. For this reason, the temperature of the mass flow into the cold storage is unknown.

To calculate the temperature T_{CS} analytically, a fix-point investigation would have to be introduced. In this case, a numerical determination of the temperature is followed. The algorithm in figure 3.13 and the corresponding table 3.6 disclose the grid-searching procedure.

To determine T_{CS}, possible values for the temperature of the cold storage have to be figured out. The algorithm iterates through the available estimate temperatures and decides upon the first solution. The possible values for the cold storage temperature are stored in the array $T_{CS,guess,vector}$ (1). The number of iterations n is equal to the length of this vector. After determining an initial cost of disproportionately high value and setting the iteration variable

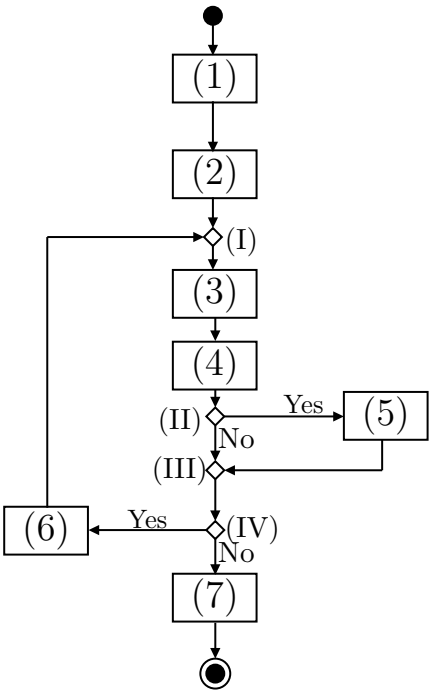

Figure 3.13: Activity diagram to determine the temperature of the cold storage numerically. The activities are listed in table 3.6

Node	Activity
(1)	Set $T_{CS,guess,vector}$
(2)	$cost_{initial} = \infty, i = 0$
(I)	Decision node
(3)	$T_{CS,actual} = f(T_{CS,guess,vector}[i])$
(4)	$cost = \lvert T_{CS,actual} - T_{CS,guess,vector}[i] \rvert$
(II)	$cost < cost_{initial}$?
(5)	$cost_{initial} = cost$, $T_{CS,solution} = T_{CS,guess,vector}[i]$
(III)	Decision node
(IV)	$i < n - 1$?
(6)	$i = i + 1$
(7)	Return $T_{CS,solution}$

Table 3.6: The table corresponding to figure 3.13 to determine the cold storage temperature

i to zero (2), the first equation is solved. The ordinary differential equation 3.35 is solved by setting the estimated value of the cold storage as the temperature of the mass inflow (3).

In the next step, the deviation of the actual temperature, which is attained from solving the integral, and the estimated temperature, is determined (4). If this error is smaller than the initial one, it overwrites the initial cost. Then, the estimated temperature is defined as $T_{CS,solution}$ (5). As long as the maximum number of iterations is not reached, the procedure

is repeated (6). The entry of the temperature array $T_{CS,guess,vector}$, which shows the least deviation to the actual temperature, is returned as the optimal solution for the cold storage temperature (7).

Through this algorithm, the sub-coordinator can attain the temperature of the cold storage. Furthermore, the sub-coordinator can determine the constraint costs, which arise for the cold storage (cf. eq. 3.44). In essence, the sub-coordinator of the HPS determines $T_{CO,out}$ to minimize the cost function 3.46.

$$cost_{HPS}\left(T_{CO,out}\right) = a \cdot cost^{b}_{cons,HPS} + c \cdot cost^{d}_{cons,HPS} \cdot cost_{operation,HPS} + cost_{operation,HPS} \tag{3.46}$$

After minimizing this cost function, the sub-coordinator returns the attained value of the cost to the coordinator. Furthermore, the coordinator receives the optimization variable $T_{CO,out}$ from the sub-coordinator. In addition to the optimization variable and the cost, the actual temperature of the upper part of the heat storage $T_{HS,out,act}$ is transferred.

Approximation of the HPS

Although the sub-coordinator only has one optimization variable, the grid-searching procedure to determine the cold storage temperature is computationally complex. To reduce the computing time, an approximation of the cost function is introduced. The temperature of the heat and the cold storage have time-changing dynamics. Therefore, a stationary energy balance of the HPS would not lead to a reasonable representation of its behavior. For this reason, the cost function of the heat-pump-system is approximated through a parametric programming approach. In this parametric programming approach, the costs of the HPS are obtained, stored, and finally approximated through an interpolation.

The sub-coordinator of the heat-pump-system receives the mass flows $\dot{m}_{CS}$ and $\dot{m}_{HS}$ and their temperatures $T_{CS,in}$ and $T_{HS,in}$ as parameters. Furthermore, the values of $T_{ambient}$, $\dot{m}_{CO}$, and $\dot{m}_{EV}$ are transferred. These parameters are treated as constants during the interpolation. The values of these parameters are average values from the simulation of the energy system and are listed in table 3.7.

Furthermore, the coordinator hands over the initial temperature of the heat storage, the initial temperature of the cold storage, and the set-variable $T_{HS,out,set}$ to the sub-coordinator of the HPS. Since these values are time-varying, different values have to be considered. Therefore, a range of values for the temperatures $T_{HS,out,set}$, $T_{HS,initial}$ and $T_{CS,initial}$ is introduced in table 3.8.

Parameter	Value
$\dot{m}_{CS}$	14 kg s^{-1}
$\dot{m}_{HS}$	1 kg s^{-1}
$\dot{m}_{CO}$	16 kg s^{-1}
$\dot{m}_{EV}$	11 kg s^{-1}
$T_{CS,in}$	285 K
$T_{HS,in}$	298 K
$T_{ambient}$	283 K

Table 3.7: Constant parameters for the interpolation of the HPS

Parameter	T_{min}	T_{max}
$T_{HS,initial}$	297 K	313 K
$T_{CS,initial}$	277 K	293 K
$T_{HS,out,set}$	297 K	313 K

Table 3.8: Range of the varying parameters for the interpolation of the HPS

The variables $T_{HS,out,set}$, $T_{HS,initial}$ and $T_{CS,initial}$ are discretely varied within their respective ranges. In essence, 512 optimizations are performed by the sub-coordinator with different combinations of these variables. The resulting costs are saved and the approximate cost function $\widetilde{f}$ (cf. eq. 3.47) is obtained through linear interpolation.

$$cost_{HPS,approx} = \widetilde{f}\left(T_{HS,initial}, T_{CS,initial}, T_{HS,out,set}\right) \tag{3.47}$$

3.4 Coordinator

The coordinator is the regulating instance of the hierarchical multi-agent-system. It possesses the highest decision-making capability and, therefore, controls the activities of its subsystems.

Figure 3.14 represents the coordinator's point of view of the considered energy system. The coordinator has an interface to the HTS, the HXS, the HPS, and both consumers. The decision variables of the coordinator are the input temperature of the first consumer $T_{C1,in}$, the input temperature of the second consumer $T_{C2,in}$, and the output temperature of the heat-pump-system $T_{HPS,out}$. Consequently, the coordinator manipulates these input variables to locate the global minimum of its cost function 3.48.

$$cost\left(T_{C1,in}, T_{C2,in}, T_{HPS,out}\right) = cost_{C1} + cost_{C2} + cost_{HTS,approx} + cost_{HXS} + cost_{HPS,approx} \tag{3.48}$$

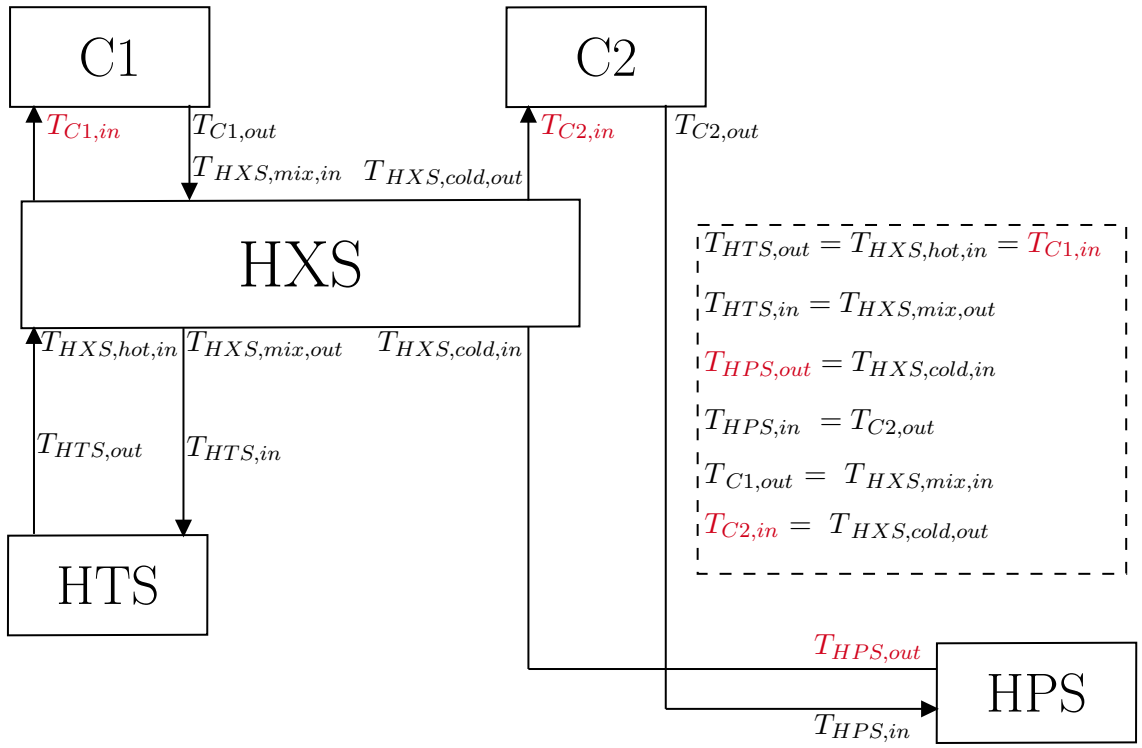

Figure 3.14: The coordinator's point of view of the considered energy system
Optimization variables of the coordinator: $T_{C1,in}$, $T_{C2,in}$ and $T_{HPS,out}$
The coordinator optimizes the interaction of all subsystems. The optimization variables of the coordinator are displayed in red. The equations in the dashed box show the dependency and interaction of the system variables.

The temperature, which enters the first consumer, is equal to the temperature leaving the HTS and entering the hot part of the HXS. Furthermore, the input temperature of the HTS results from the mix-temperature, which leaves the HXS. The HXS receives the optimization variable $T_{HPS,out}$ as an input variable. Moreover, the HXS causes the input temperature of the second consumer. Also, the exiting mass flow of the second consumer and its temperature serve as input variables for the HPS. These interactions are regulated by the coordinator. Moreover, the coordinator optimizes its composed cost function to initiate an optimized operation of the considered energy system.

First of all, the coordinator determines the optimal coupling variables through minimization of the approximated cost function 3.48. Afterwards, the coordinator hands over the resulting coupling variables to the sub-coordinators of the subsystems. Then, the sub-coordinators optimize the operation of their subspace, while simultaneously fulfilling the submitted coupling variables by the coordinator. Furthermore, the coordinator receives the set-variables for the agents' components, which are determined by the respective sub-coordinator.

With the determination of the cost-minimizing set-variables of the components, the hierarchical multi-agent optimization procedure is completed. As mentioned in section 3.1.1, the multi-agent-system's objective is to transfer the attained optimal set-variables to the control instance. Then, the optimal control sequence is initiated for the pending time interval.

3.4.1 MPC Algorithm

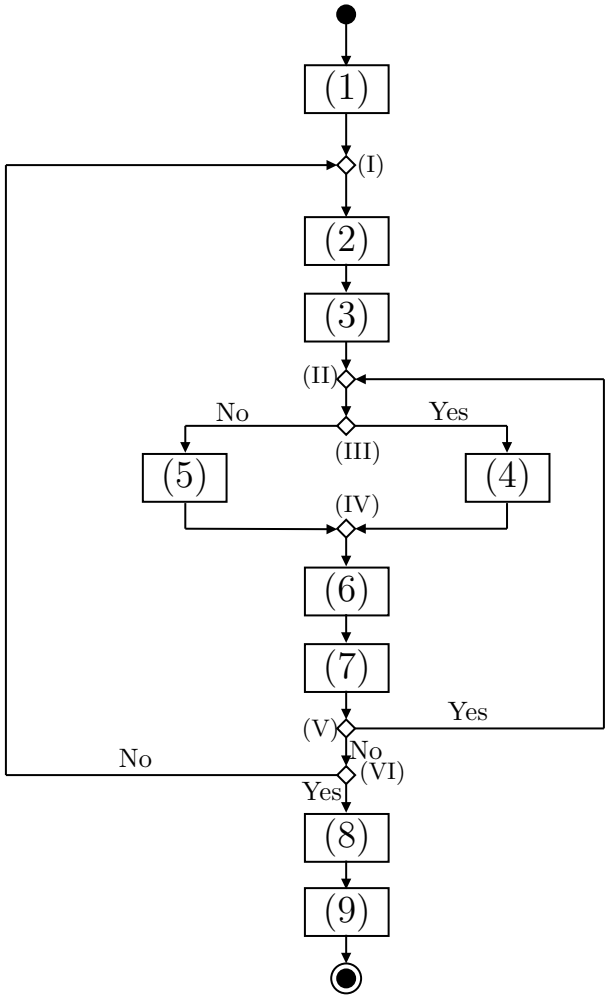

Figure 3.15: Activity diagram to describe the MPC algorithm applied by the coordinator. The corresponding activities are listed in table 3.9

To enhance the operational optimization, the coordinator can consider future events. Therefore, the decision variables $T_{C1,in}$, $T_{C2,in}$ and $T_{HPS,out}$ should not only be chosen to optimize the operation of the next time step. The optimization variables should initiate an optimized control sequence for the whole prediction horizon. Accordingly, the coordinator makes use

Node	Activity
(1)	Define the MPC parameters N_c and N_p
(I)	Decision node
(2)	$cost_{MPC} = 0$, $i = 0$
(3)	Define $\mathbf{x}_{opt,matrix}$, $\mathbf{x}_{opt,matrix} \in \mathbb{R}^{N_c \times n}$
(II)	Decision node
(III)	$i < N_c - 1$?
(4)	$\mathbf{x}_{opt,vector} = \mathbf{x}_{opt,matrix}[i]$
(5)	$\mathbf{x}_{opt,vector} = \mathbf{x}_{opt,matrix}[N_c - 1]$
(IV)	Decision node
(6)	$cost_{MPC} = cost_{MPC} + cost\,(\mathbf{x}_{opt,vector}, time)$
(7)	$time = time + \delta t$, $i = i + 1$
(V)	$i < N_p - 1$?
(VI)	Global minimum or maximum number of iterations reached?
(8)	$\mathbf{x}_{opt,vector} = \mathbf{x}_{opt,matrix}[0]$
(9)	Hand over $\mathbf{x}_{opt,vector}$ to the sub-coordinators

Table 3.9: Activity diagram of the MPC algorithm, corresponding to 3.15.

of model predictive control (cf. sec. 2.3) to determine the cost-minimizing variables. Figure 3.15 and the corresponding table 3.9 describe the MPC-algorithm of the coordinator.

Initially, the control horizon N_c and the prediction horizon N_p have to be set (1). The prediction horizon defines, how many future sequences are taken into consideration to optimize the operation. In contrast, the control horizon determines the total number of variables, which have to be optimized by the coordinator. Furthermore, the iteration variable i and the costs for the entire prediction horizon are set to zero (2).

To illustrate the MPC-algorithm with an application example, N_p is set to three and N_c is set to two. First, the coordinator has to define a matrix (cf. eq. 3.49), which represents the coupling variables (3). These coupling variables have to be optimized by the coordinator. Since the coordinator has to determine the input temperature of the first consumer, the input temperature of the second consumer, and the output temperature of the HPS, the number of columns of $\mathbf{x}_{opt,matrix}$ is set to three. The number of rows of the optimization matrix is defined by the control horizon N_c. Therefore, the coordinator has to optimize six variables.

$$\mathbf{x}_{opt,matrix} = \begin{pmatrix} T_{C1,in,1} & T_{C2,in,1} & T_{HPS,out,1} \\ T_{C1,in,2} & T_{C2,in,2} & T_{HPS,out,2} \end{pmatrix} \tag{3.49}$$

First of all, the coordinator determines the cost of operation of the first time step (6). For this time step, the first row of $\mathbf{x}_{opt,matrix}$ is inserted into equation 3.48 (4). Comparatively, the determination of the operational costs of the second time step (7) is done with the second row of the optimization matrix.

The control horizon and, therefore, the number of rows of $\mathbf{x}_{opt,matrix}$ only amounts to two. Nonetheless, three time steps have to be considered. For this purpose, the coupling variables of the last time step of the prediction horizon are set equal to the coupling variables of the last time step of the control horizon. Therefore, the coordinator adopts the variables of the second row of the optimization matrix and inserts these variables into its cost function 3.48, to determine the cost value for last time step of the prediction horizon (5). The individual costs of each time step are added up (6). The costs of the entire prediction horizon are represented by equation 3.50.

$$cost_{MPC} = cost(t_1) + cost(t_2) + cost(t_3) \tag{3.50}$$

The coordinator's objective is to determine the global minimum of the cost function 3.50. In this case, the global optimization procedure is executed with six variables, whose optimal values have to be identified. Even though the variables for the entire control horizon are optimized, only the coupling variables for the first step are implemented. Therefore, the optimization vector in equation 3.51 is adopted and identified as the control action, which initiates an optimal operation (8). This vector is transferred from the coordinator to the respective sub-coordinator (9).

$$\mathbf{x}_{opt,vector} = \begin{pmatrix} T_{C1,in,1} & T_{C2,in,1} & T_{HPS,out,1} \end{pmatrix} \tag{3.51}$$

The implementation of $\mathbf{x}_{opt,vector}$ not only leads to an optimized operation of the next time step; it initiates an optimal operation for the entire prediction horizon. The other obtained, optimal coupling variables are not implemented. Though, they can be utilized as the initial optimization values for the next time step.

3.5 Implementation

The illustration in 3.16 is the UML-diagram of the object-oriented implementation of the hierarchical multi-agent-system. First, a cost-function-generator-class (cfg) is created. This class contains the equations to determine the thermal costs, the energy cost, the emission costs and the lifetime-reduction costs. Furthermore, the cost-function-generator-class acts as the parent-class for the cfg-provider and the cfg-user. Users only have thermal costs. In contrast, providers contain functions for the energy costs, the emission costs and the lifetime-reduction costs. The cost functions of the boilers, the CHP, the heat pump, the heat exchanger, and the pump inherit from cfg-provider. Moreover, the cfg of the consumer is the sub-class of cfg-user.
The agent-class is the parent-class of every implemented agent in this work. Furthermore, the

agent-class creates objects of the cfg-units of the agents. Therefore, agents have the ability to determine their cost value.
Moreover, the sub-coordinator-class creates objects of the implemented agents. It acts as the parent class of the sub-coordinators of the HTS, the HXS, and the HPS.
The coordinator creates an object of every subsystem, that has a direct connection to the coordinator (cf. fig. 3.5). Therefore, each sub-coordinator and the agents of both consumers are objects in the class of the coordinator. Since no child-class inherits from the class of the coordinator, it is not illustrated in the UML-diagram 3.16.

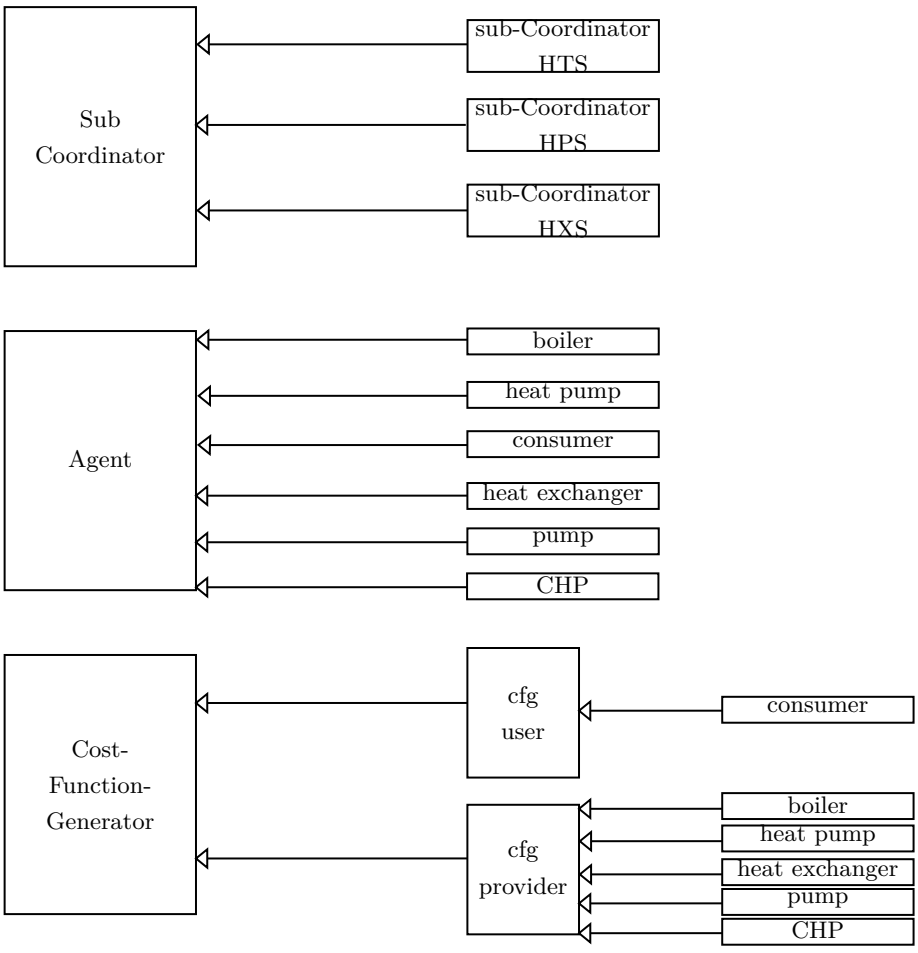

Figure 3.16: UML-diagram of the agent-based implementation

4 Results and Evaluation

This chapter presents and discusses the results of the developed agent-based system. The operational optimization with the multi-agent-system is applied to the E.ON ERC main building in a simulation.
All experiments are simulated on an Intel Core i7 processor with two cores, four logical processors, and 8 GB of random-access memory. The hierarchical multi-agent-system is implemented in Python. Moreover, the environment for the simulation of the energy system is modeled in Modelica. The Modelica-model of the main building energy system is exported to a functional mock-up unit in Python. Therefore, the simulations are run in Python.

In section 4.1, the approximated cost function approach of the HTS (cf. fig. 3.2) is compared to an iterative approach. Furthermore, the optimization of the entire considered energy system is investigated in section 4.2.

To evaluate and compare simulations, different criteria are considered. For instance, the input temperature of the consumers has to be analyzed. Therefore, the fulfillment of the set-temperature is evaluated. Besides the visual assessment of the temperature profile, a key performance indicator is utilized. As the key performance indicator for the control quality of the temperature, the root mean square error (RMSE) is introduced [Hora and Campos, 2015]. The RMSE is calculated through function 4.1.

$$\mathrm{RMSE} = \sqrt{\frac{1}{N_{fev}} \sum_{i=1}^{N_{fev}} e_i^2} \tag{4.1}$$

The expression of the RMSE contains the number of function evaluations N_{fev} and the control deviation e. In this case, the control deviation is the difference between the desired and the actual input temperature of the consumer. To reduce the influence of the transient phase, the first six hours of the simulations are neglected in the calculation of the RMSE.

Table A.2 in the appendix summarizes the settings of the simulations. This table contains values for the number of iterations each optimizing instance has implemented. Furthermore, the time interval δt is listed. The parameter δt does not only influence the cost functions; it also determines the number of optimizations per hour of simulation. Correspondingly, after every time interval δt, the agent-based optimization instance is invoked and an operational optimization is performed.

The presented simulations employ an MPC-procedure (cf. sec. 3.4.1), which only considers the first time-step. Hence, N_p and N_c are set equal to one.

4.1 Comparison of the Approximated and the Iterative Optimization

To compare the approximated and the iterative optimization scheme of the HTS-optimization, a simulation with both approaches is established. If the simplified cost function is not employed, the sub-coordinator of the HTS would have to minimize its cost function (cf. eq. 3.18) before transmitting the determined costs to the coordinator. Afterward, the coordinator chooses new set-points for the coupling variables, whereupon the sub-coordinator starts a new minimization of the cost function. This procedure is repeated until the optimal value for the coupling variables is found. A concurrent optimization by the sub-coordinators would lead to an iterative determination of the optimal coupling variables of the subsystems (cf. fig. 3.2).

To compare both approaches, only the HTS and the first consumer are investigated in a simulation of the first five days of the year. In both cases, the first consumer desires an input temperature of 345 K. The temperature profile and the required simulation time of the approximated and the iterative approach are compared to each other.

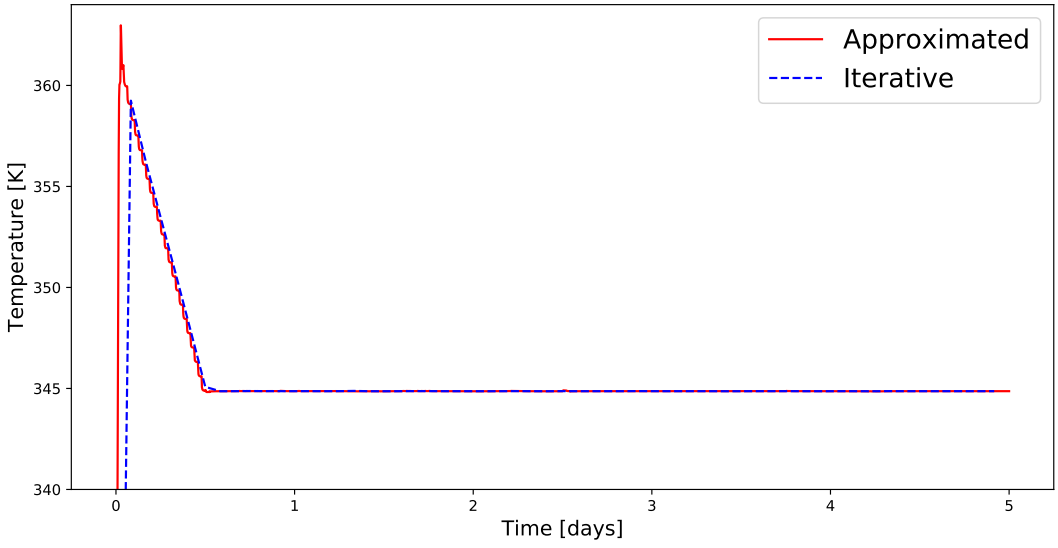

Figure 4.1: Temperature profile of the first consumer. The optimization with the approximation is represented by the red solid line. The iterative approach is shown by the blue dashed line.

Figure 4.1 shows the temperature profile for the first consumer. The red solid line represents the results of the approximated simulation, whereas the blue dashed line belongs to the iteratively obtained values. As can be seen, apart from the transient phase, the temperature profiles of both approaches are identical. Besides the visual similarity of the temperature profiles, the values of the RMSE resemble each other. The RMSE of the approximated approach is 1,00, whereas the value for the iterative approach is only 3 % higher. (cf. tab. 4.1).

In contrast to the obtained similarity in the temperature profile, the approaches show significant disparities, when it comes to the computational complexity. The approximated approach needs twelve minutes of computing time to execute the five-day simulation. Different from the simplified optimization, the iteratively obtained results take 19 hours to complete the required simulation (cf. tab. 4.1).

In essence, the introduction of the approximated cost representation of the HTS leads to a compelling decrease in computational complexity, while simultaneously providing the same results. For this reason, the remaining simulations contain the approximated optimization approach of the HTS.

Parameter	Approximated Optimization	Iterative Optimization	Relative Value
RMSE (T_1)	1,00	1,03	0,97
Simulation time	0,2 h	19 h	0,01

Table 4.1: Simulation results for the approximated optimization and the iterative optimization. The relative values are attained through scaling the approximated value with the values of the iterative optimization.

4.2 Optimized Operation

The developed multi-agent-system introduces an operational optimization of the energy system (cf. fig. 3.14). The simulations in this section are made for the first seven days of the year.

4.2.1 Optimized Operation and Reference Control

To evaluate the performance of the operational optimization, the introduced operational optimization is compared to the reference control. The following simulations consider the optimization of the HTS, the HXS, the HPS, the first consumer, and the second consumer. First, the temperature profiles of both consumers are considered. Moreover, a detailed analysis of the energy consumption is presented. Finally, the energy costs are compared. Since the coordinator minimizes its cost function on a monetary basis, the attained costs offer the most profound expressiveness. Besides the graphical illustrations, the displayed values are summarized in table 4.2 at the end of this section.

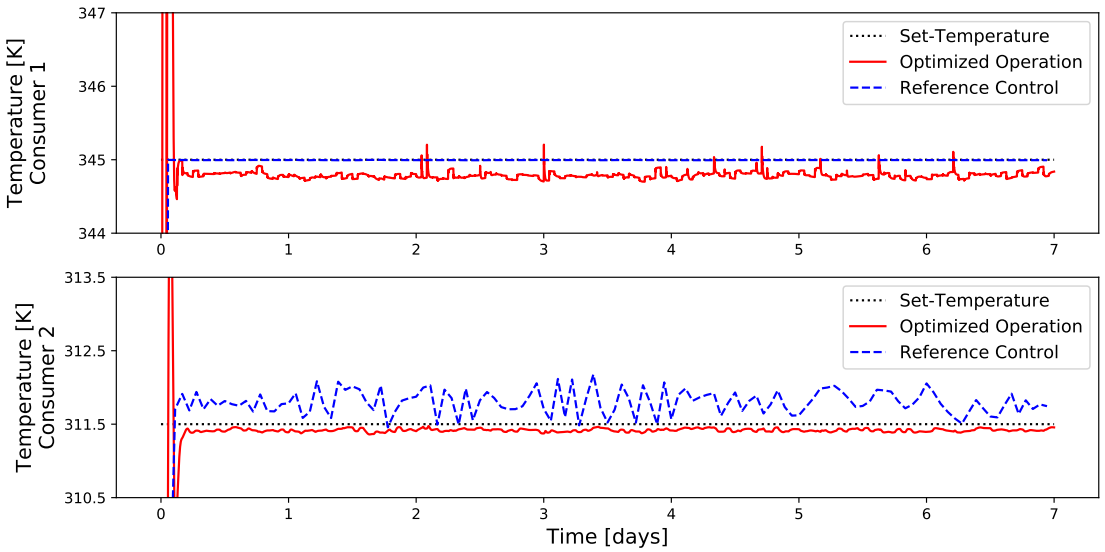

Figure 4.2: Temperature profiles of the first consumer (upper) and the second consumer (lower).
The optimized operation (red solid line) is compared to the reference control (blue dashed line). The desired set-temperature of the consumers is represented by the black dotted line.

The provided figure 4.2 represents the temperature profiles of the first and the second consumer for the optimized operation and the reference control. The upper sub-figure shows the

temperature profile of the first consumer. The desired set-temperature of 345 K is illustrated by the black dotted line. As can be seen, the desired temperature of 345 K is held accurately by the reference control. The temperature profile of the optimized operation is below the desired input temperature of the first consumer. However, the deviation is rather small. The temperature distinction occurs due to the implemented allowed temperature deviation δT_{dev} of 0,1 K (cf. tab. A.2). Furthermore, heat losses, which occur inside the pipelines, are neglected during the operational optimization. The RMSE of the optimized operation is about twice the RMSE of the reference control. Besides the slightly lower temperature of the optimized operation, the transient phase is decisive for the difference of the RMSE.

The temperature curves of the second consumer, which are illustrated on the lower sub-figure of graphic 4.2 show, that the reference control oscillates significantly from the desired set-temperature of 311,5 K. The increased quality in control of the optimized operation is further underlined by the meaningful difference of the RMSE (cf. tab. 4.2).
The reference control predominantly uses the heat pump to supply the second consumer. The heat pump of the reference control is permanently switched on and off. Therefore, the supplied heat from the heat pump to the heat storage oscillates. Because of the oscillating heat pump and the inert behavior of the heat storage, the temperature of the heat storage and, therefore, the input temperature of the second consumer oscillate as well.

The cost function of the coordinator of the optimized operation (cf. eq. 3.48) contains the costs transferred by the consumers. Therefore, the coordinator attempts to minimize the penalization of the consumers. The reference control does not contain any costs for a temperature deviation. For this reason, the distinction in control quality arises.

After analyzing the temperature profiles of both approaches, the energy consumption is considered. The bar chart in 4.3 compares the electricity values of the optimized operation and the reference control. Especially the amount of generated electricity differs significantly between both control strategies. While the reference control generates 123 kWh of electricity in seven days, the optimized operation generates more than twelve times the amount. Besides the increase in electricity generation, the optimized operation has decreased electricity consumption. The optimized approach consumes 1.737 kWh of electricity, whereas the reference control uses 3.102 kWh. Furthermore, the optimized operation only employs 11 % of input energy for the heat pump when compared to the reference control.

The optimized operation introduces the opportunity to transfer heat from the HTS to the cold part of the energy system. This transfer is executed inside of the HXS (cf. eq. 3.22). Moreover, the increased electricity generation by the CHP and the decreased electricity consumption by the heat pump indicate, that the coordinator chooses to use the HTS to increase the temperature of the mass flow exiting the HPS. Therefore, the HTS is exploited more by the optimized operation.

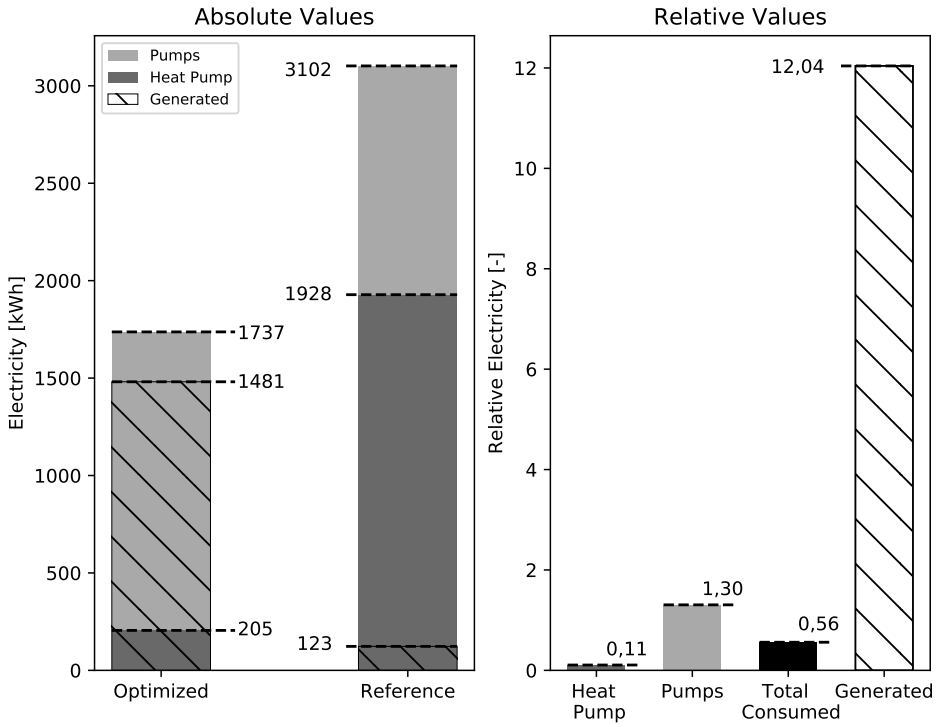

Figure 4.3: Consumed electricity and generated electricity of the optimized operation and the reference control.
The electricity consumption comes from the pumps and the heat pump. The CHP enables an electricity generation. The relative values on the right subfigure are attained through scaling the values of the optimized operation with the values of the reference control.

The increase in gas consumption by the HTS is illustrated in graphic 4.4. Especially the CHP is used more during the simulation of the optimized operation. The CHP consumes 6.048 kWh of natural gas for the optimized operation, while the reference control only requires 715 kWh. Since the increase in CHP usage correlates with the increase in electricity generation (cf. fig. 4.3), the coordinator recognizes the potential to generate electricity when utilizing the CHP. This behavior is represented in the cost function of the CHP (cf. eq. 3.4), which contains a benefit-factor for the generated electricity. Therefore, the penalization of utilizing the CHP decreases significantly.
Besides the CHP, the boilers are also exploited more compared to the reference control. In essence, the optimized operation consumes six times more gas than the reference control. While the reference control requires 2.179 kWh of natural gas, the simulation of the optimized operation shows a need for 13.083 kWh for seven days.

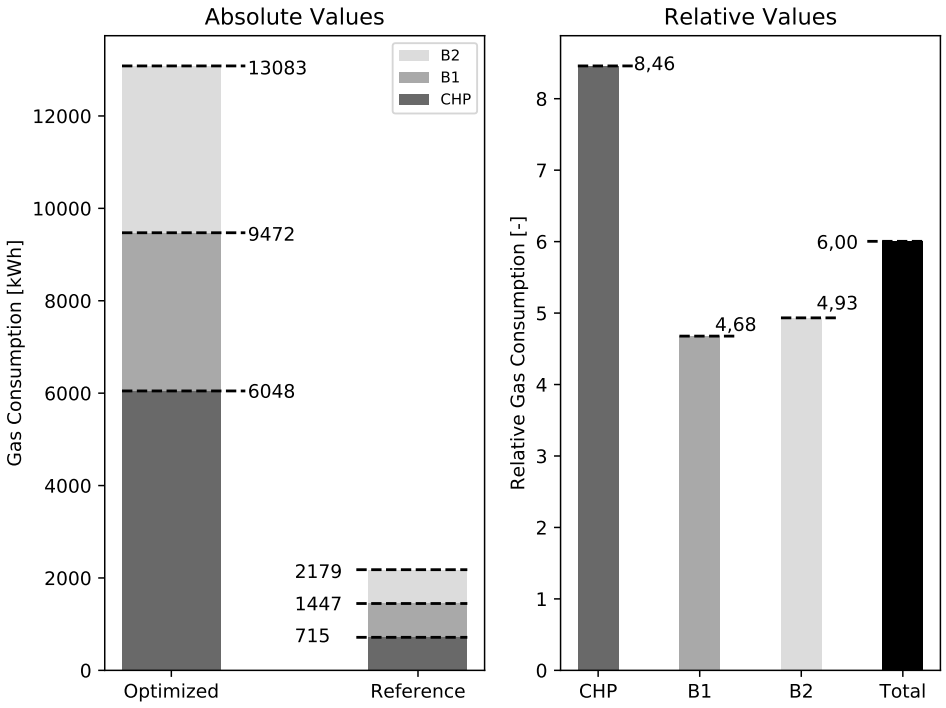

Figure 4.4: Gas consumption of the optimized operation and the reference control. Gas is consumed by the boilers and the CHP. The relative values on the right sub-figure are attained through scaling the values of the optimized operation with the values of the reference control.

The values for the energy consumption show, that the coordinator exploits the HTS significantly more than the HPS. It has to be stated, that the implemented operational optimization assumes constant efficiencies of the components. Therefore, a decrease in thermal efficiency with increasing temperature is not implemented. Especially the coefficient of performance of the heat pump (cf. 3.7) changes significantly when operated on different temperature levels [Müller, 2019b]. Different values for the efficiencies, changing energy prices, or temperature-dependent modeling of the components is not considered in this work.

Since the operational optimization aims to reduce a cost function on a monetary basis, its impact has to be evaluated with the inclusion of energy costs. Figure 4.5 compares the costs for the optimized operation and the reference control. The increased usage of the HTS is underlined by significantly higher gas costs. With 785 MU, the gas costs of the optimized operation are six times higher in contrast to the reference control. Despite the increase in gas costs, the higher electricity generation and lessened electricity consumption cause a

compelling reduction in electricity costs. Therefore, the electricity costs of the optimized operation only amount to 14 %, when compared to the reference control. Altogether, the optimized operation introduces a decrease in total energy costs of 15 % and only causes 918 MU in total energy costs. The reference control, on the other hand, requires 1.079 MU. The reduced energy costs and the significant increase in control quality of the temperature of the second consumer (cf. fig. 4.2) show, that the implemented operational optimization can convert its requirements, which are stated as cost functions, into the simulation, and optimize the operation accordingly.

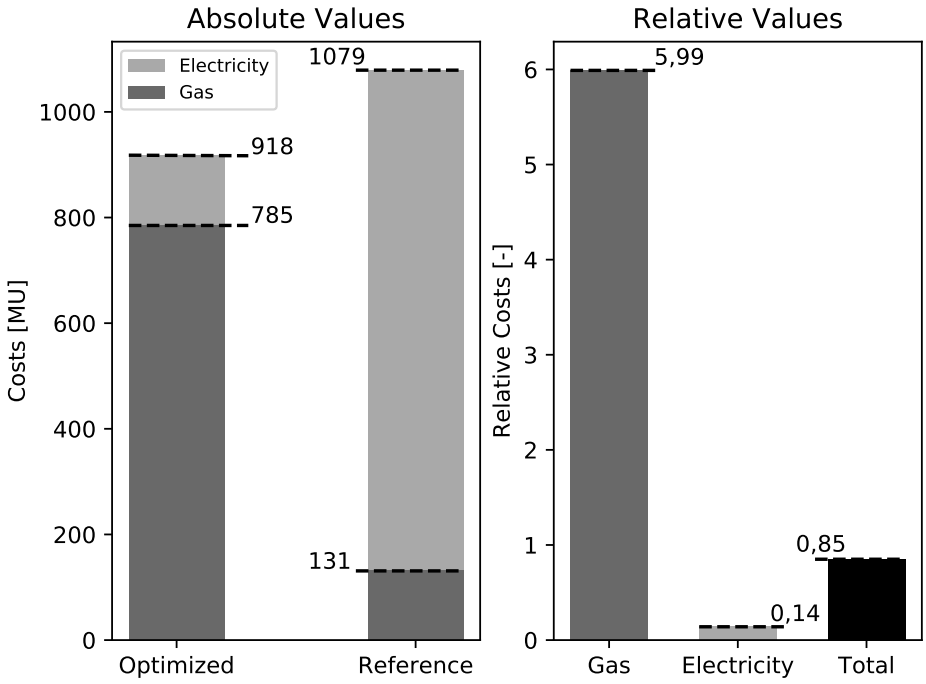

Figure 4.5: Energy cost of the optimized operation and the reference control.
The total cost is composed of gas costs and electricity costs. The relative values on the right sub-figure are attained through scaling the values of the optimized operation with the values of the reference control.

Parameter	Optimized Operation	Reference Control	Relative Value
RMSE (T_1)	0,21	0,10	2,10
RMSE (T_2)	0,10	0,32	0,31
Gas consumption CHP	6.048 kWh	715 kWh	8,46
Gas consumption Boiler 1	3.424 kWh	732 kWh	4,68
Gas consumption Boiler 2	3.611 kWh	732 kWh	4,93
Total gas consumption	13.083 kWh	2.179 kWh	6,00
Electricity consumption pumps	1.532 kWh	1.174 kWh	1,30
Electricity consumption heat pump	205 kWh	1.928 kWh	0,11
Total electricity consumption	1.737 kWh	3.102 kWh	0,56
Total energy consumption	14.820 kWh	5.281 kWh	2,81
Electricity generation	1.481 kWh	123 kWh	12,04
Gas costs	785 MU	131 MU	6,00
Electricity costs	133 MU	948 MU	0,14
Total costs	918 MU	1.079 MU	0,85

Table 4.2: Simulation results for the optimized operation and the reference control. The relative values are attained through scaling the values of the optimized operation with the values of the modified reference control.

4.2.2 Optimized Operation and Modified Reference Control

The most significant difference between the optimized operation and the reference control is the usage of the CHP and, therefore, the amount of generated electricity (cf. fig. 4.4, 4.3). The following experiment attempts to investigate, whether the distinct usage of the CHP is the reason why the optimized approach causes fewer energy costs. Therefore, a modified reference control is introduced, which only employs the CHP to increase the temperature within the HTS. Moreover, the temperature profile of the first consumer and the operational costs of the optimized operation are compared to the modified reference control.

Graphic 4.6 demonstrates the temperature profile of the first consumer for the optimized operation and the modified reference control, respectively. Since the operation of the HPS of the modified reference control is identical to the non-modified one, the temperature profile of the second consumer is not investigated any further in this section.
The temperature profile of the modified reference control comes close to the desired temperature of 345 K of the first consumer. Moreover, a low RMSE of 0,17 (cf. tab. 4.3) underlines this assumption. Therefore, it can be stated, that the usage of the CHP is sufficient to reach the desired temperature of the first consumer accurately enough.

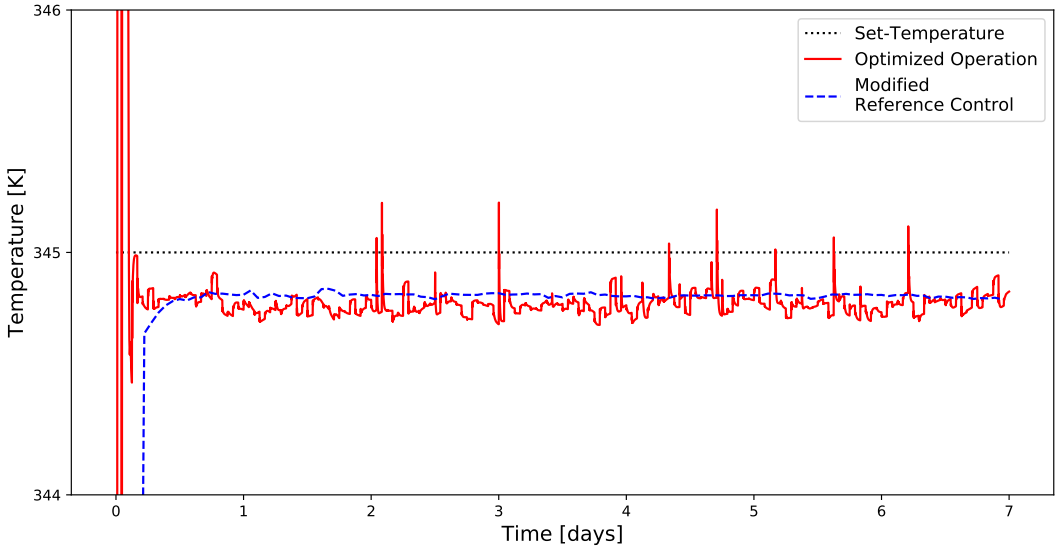

Figure 4.6: Temperature profile of the first consumer.
The optimized operation (red solid line) is compared to the modified reference control (blue dashed line). The modified reference control only employs the CHP to heat the HTS. The desired set-temperature of the consumer is represented by the black dotted line.

The energy costs of the optimized operation and the modified reference control are compared in the bar chart 4.7. The simulation with the modified reference control has 160 MU in gas costs, which is approximately five times less when compared to the optimized operation. Nevertheless, the optimized operation only causes 16 % of the electricity costs. In total, the optimized operation can save 7 % of the total cost, when compared to the modified reference control.

Figure 4.5 in section 4.2 shows a cost difference of 15 %. Therefore, 8 % of the operational costs can be saved, when only using the CHP in the HTS. However, the remaining cost reduction of 69 MU is not caused by this modification. Therefore, it can be stated, that the usage of the CHP is not the only reason why the optimized approach causes fewer energy costs than the reference control. Besides the increased usage of the CHP, the heat transfer from the hot side to the cold side of the energy system is indispensable, when minimizing the operational costs.

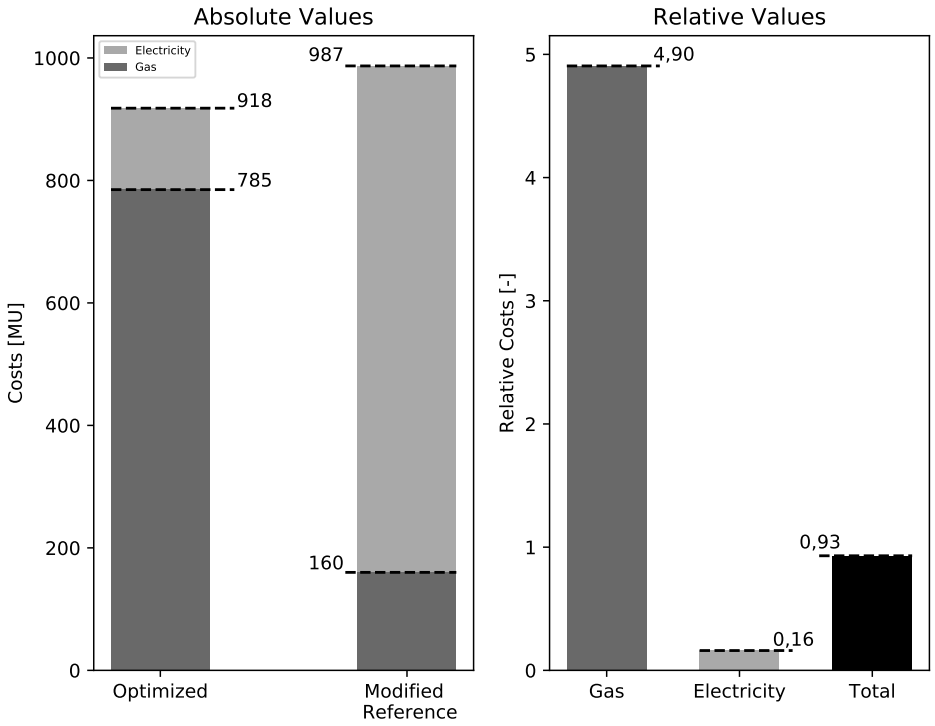

Figure 4.7: Energy cost of the optimized operation and the reference control. The total cost is composed of gas costs and electricity costs. The relative values on the right sub-figure are attained through scaling the values of the optimized operation with the values of the modified reference control.

Parameter	Optimized Operation	Modified Reference Control	Relative Value
RMSE (T_1)	0,21	0,17	1,24
RMSE (T_2)	0,10	0,32	0,31
Gas costs	785 MU	160 MU	4,91
Electricity costs	133 MU	827 MU	0,16
Total costs	918 MU	987 MU	0,93

Table 4.3: Simulation results for the optimized operation and the modified reference control. The relative values are attained through scaling the values of the optimized operation with the values of the modified reference control.

4.2.3 Optimized Operation with Modified Consumer Behavior

The cost function of the consumer (cf. eq. 3.12) includes the parameter RPE. The RPE explicitly depends on δT_{dev}, which defines the allowed temperature deviation without causing any thermal costs (cf. eq. 2.11). This experiment is simulated with an allowed temperature deviation of 2 K (cf. tab. A.2). Furthermore, the number of people affected per consumer-unit n_p is reduced to five. The reduced number of people weakens the caused thermal costs (cf. eq. 2.11). Overall, this simulation's objective is to assess, whether the coordinator still attempts to reach the set-temperature of the consumers, despite the reduced thermal penalty. Additionally, the effect of δT_{dev} is investigated. Due to the increased range of non-penalizing temperature deviation, the coordinator can decrease or increase the temperature of the consumers in this range and not cause any thermal costs. To evaluate these points, the temperature profiles and the energy costs of the optimized operation and the optimized operation with modified consumer behavior are evaluated.

The upper part of the supplied graph in 4.8 presents the temperature profiles of the first consumer. In contrast to the normal optimized operation, the modified optimized operation deviates significantly from the initial set-temperature of 345 K. The deviation is further emphasized by the value of the RMSE (cf. tab. 4.4). Therefore, the coordinator recognizes the potential to provide the consumer with 2 K less than the desired temperature, without causing thermal costs. The increased amplitude of the temperature profile is also caused by an increased range of non-penalized temperature divergence. Nevertheless, the coordinator still aims to satisfy the comfort demands of the consumer, despite the reduced number of affected people.

The same principles apply to the lower part of figure 4.8, which shows the temperature profile of the second consumer. On the one hand, the set-temperature of 311,5 K is held approximately accurate by the normal optimized control (red line). On the other one, the average temperature of the optimized operation with modified consumer behavior amounts to about 309,5 K, which is 2 K less than the desired temperature of the second consumer.
In summary, the coordinator can recognize the changed consumer behavior and exploit the arising advantages.

Figure 4.9 illustrates the energy costs for both approaches. In comparison to the normal optimized operation, the optimized operation with modified consumer behavior can save 7 MU in energy costs. The cost-saving results from the reduced input temperature of the consumers.
The optimized operation with modified consumer behavior requires 2 % less in gas costs when compared to the normal optimized operation. However, the electricity cost is 6 MU higher for the optimized operation with modified consumer behavior. The increase in electricity cost is caused by the increased usage of the heat pump (cf. tab. 4.4). The optimized operation with

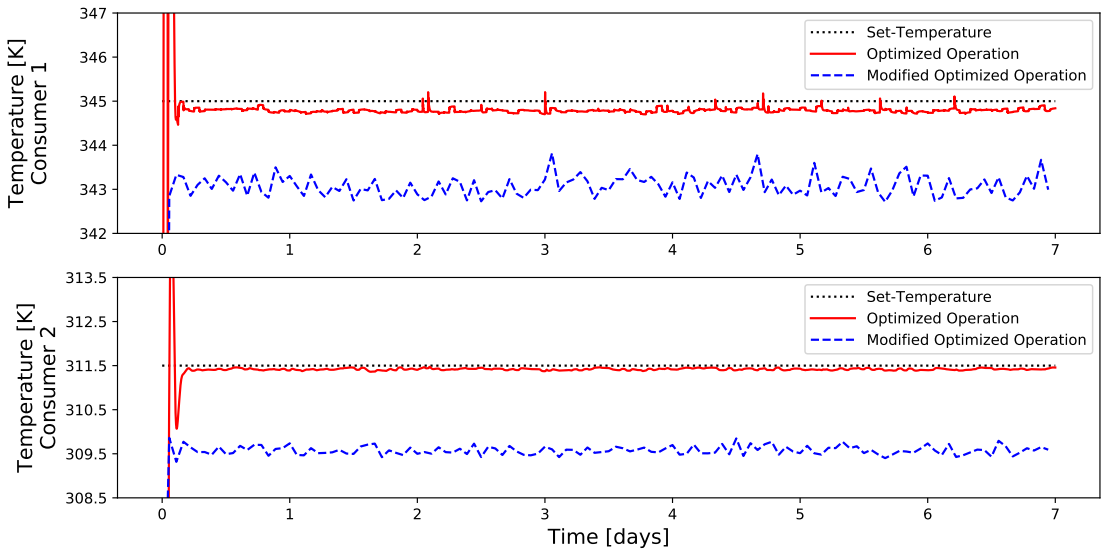

Figure 4.8: Temperature profiles of the first consumer (upper) and the second consumer (lower). The normal optimized operation (red solid line) is compared to the optimized operation with modified consumer behavior (blue dashed line). The modified consumer behavior has an extended range of non-penalizing temperature deviation. The desired set-temperature of the consumers is represented by the black dotted line.

modified consumer behavior requires 27 kWh of input energy more into the heat pump when compared to the normal optimized operation. The increase in heat pump utilization indicates, that less heat is transferred through the HXS to heat the mass flow, that reaches the second consumer. Although the optimization's objective is achieved and the total energy costs are reduced, an increase in heat pump usage contradicts the expectations, when supplying less energy to the consumers.

This result discloses a weakness of the introduced operational optimization. The dynamics of the heat-pump-system are obtained from the energy system, which supplies the second consumer with an input temperature of 311,5 K. The input temperature influences the output temperature, which is seen as a constant parameter during the interpolation of the HPS (cf. tab. 3.7). Besides the parameters for the interpolation, the behavior of the storages (cf. eq. 3.37 - 3.40) is determined for a constant operation of the cold part of the considered energy system. Changing dynamics of the cold side of the energy system are not considered while modeling and approximating the HPS. This leads to minor changes in the coordinator's optimization. However, the effect of the changing dynamics is not investigated any further in this work.

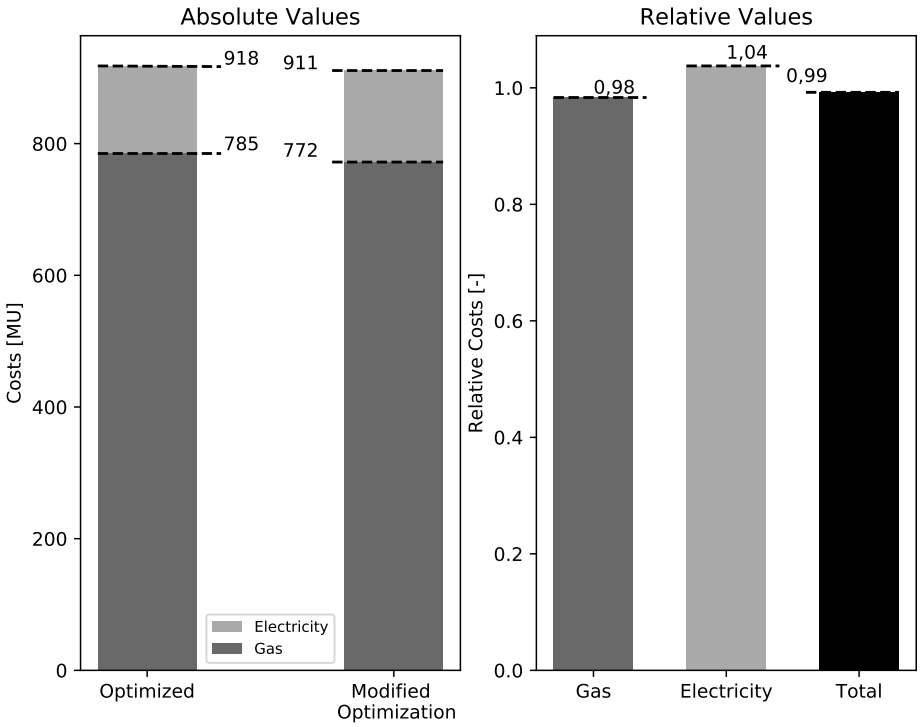

Figure 4.9: Energy cost of the optimized operation and the optimized operation with modified consumer behavior.
The total cost is composed of gas costs and electricity costs. The relative values on the right sub-figure are attained through scaling the values of the optimized operation with modified consumer behavior with the values of the optimized operation with normal consumer behavior.

Parameter	Optimized Operation	Modified Optimized Operation	Relative Value
RMSE (T_1)	0,21	1,86	0,11
RMSE (T_2)	0,10	1,86	0,05
Electricity consumption heat pump	205 kWh	232 kWh	1,13
Gas costs	785 MU	772 MU	0,98
Electricity costs	133 MU	139 MU	1,04
Total costs	918 MU	911 MU	0,99

Table 4.4: Simulation results for the Optimized Operation and Modified Optimized Operation
The relative values are attained through scaling the values of the modified optimized operation with the values of the optimized operation.

5 Summary and Outlook

A hierarchical multi-agent-system was developed in this work to optimize the operation of an energy system. The implemented operational optimization was validated through a simulation of the E.ON ERC energy system. The validations contained comparisons of temperature profiles, energy consumption, and energy costs.

The research of hierarchical multi-agent-systems showed, that the operational optimization was mainly applied to a rather small energy system. Furthermore, the cost function of the coordinating instances usually contained energy costs and a penalty function, which was introduced for temperature deviation. An approach, that puts individual components of the cost function into relation quantitatively, was not presented for a multi-agent-system. Additionally, implemented hierarchical multi-agent-systems required a simulation to obtain discrete cost points. These discrete cost points were interpolated to attain the cost function.

The hierarchical multi-agent-system, which is developed in this thesis, uses a monetary cost function to enable a uniform contribution of each cost-component. The total cost function is compiled from energy costs, emission costs, thermal costs, and lifetime-reduction costs. Since the cost function is derived analytically, setting up the cost function does not require a completed simulation. Furthermore, this work considers a complex energy system. Therefore, the considered energy system is divided into the subsystems of the high-temperature-system (HTS), the heat-exchanger-system (HXS), and the heat-pump-system (HPS). The coordinator of the hierarchical multi-agent-system defines the optimal coupling variables of the subsystems to initiate an optimized operation. The subsystems are controlled by sub-coordinators. The sub-coordinators minimize their cost function to initiate an optimal operation of the agents, which are located inside the sub-coordinator's control space. To reduce the computational complexity of the optimization process, approximated cost representations are introduced.

First, the approximated cost representation of the HTS was compared to an exact iterative approach. The optimization with the approximated cost representation introduced a 95-times faster calculation while providing the same results. Furthermore, the operational optimization of the entire considered energy system was evaluated. The simulation with the implemented operational optimization enabled a cost reduction of 15 % when compared to the reference control. The main difference between the optimized operation and the reference control was the distinct usage of the CHP and, therefore, the difference in generated electricity.

As a result, the simulation with the optimized operation generated 1.481 kWh of electricity, which is about twelve times the amount, that the reference control generated. Besides the reduced energy costs, the optimized operation supplied the second consumer with a mass flow, which was significantly closer to the desired temperature, compared to the reference control. Furthermore, a simulation with a modified reference control was executed. The modified reference control only employed the CHP to heat the HTS. In comparison to the modified reference control, the optimized operation enabled a simulation, which caused 7 % fewer costs. Moreover, an optimized operation with modified consumer behavior was introduced. The coordinator was able to recognize the modified consumer behavior and supplied the consumers with a reduced input temperature. This modification enabled a cost-saving of 7 monetary units.

However, the simulation with the modified consumer behavior showed, that the HPS and its interpolation cannot react fully to changing dynamics. Therefore, an approximation of the HPS, which considers varying behavior of the consumer, should be introduced. Moreover, the developed hierarchical multi-agent-system only optimizes the operation of an extract of the energy system. Consequently, an enhancement of the operational optimization should include the entire energy system. Furthermore, the operation of the pumps should also be optimized.
This thesis only considered the optimization of the input temperature of the consumers. Hence, the system could be augmented by examining the temperature inside the consumers. This would enable the control of the output temperature of the consumers as well. A further extension would be, that the components are operated with temperature-dependent efficiencies. Moreover, the simulations in this thesis were optimized with constant prices for gas and electricity. Therefore, evaluations with different prices should be followed and their impact should be investigated.
Additionally, the benefit-factor in the cost function of the CHP is derived empirically. An instance, which supervises the current need for electricity within the energy system could offer a more realistic representation of the costs. This instance would serve as the electricity-agent of the energy system. The electricity agent would have an interface with the electricity generating and the electricity consuming units of the energy system. Therewith, the actual demand for electricity inside the system could be determined and the benefit-factor could be adapted accordingly.
Since the energy system is divided into subsystems, a parallel programming approach to optimize the subsystems would enable a significant reduction in computing time. Furthermore, an MPC-optimization with a prediction horizon and a control horizon greater than one should be introduced, to empower an optimization, that predicts future disturbances.

Bibliography

scipy.optimize.basinhopping — scipy v1.5.2 reference guide, 2020. URL https://docs.scipy.org/doc/scipy/reference/generated/scipy.optimize.basinhopping.html.

Abdul Afram and Farrokh Janabi-Sharifi. Theory and applications of hvac control systems – a review of model predictive control (mpc). *Building and Environment*, 72: 343–355, 2014. ISSN 0360-1323. doi: 10.1016/j.buildenv.2013.11.016. URL https://www.researchgate.net/publication/259514478_Theory_and_applications_of_HVAC_control_systems_-_A_review_of_model_predictive_control_MPC.

Sophia Ankel. Global warming: This is how much ice melted on earth in 23 years, 2020. URL https://www.weforum.org/agenda/2020/08/earth-ice-global-warming-uk-scientists/.

APS Arosio GmbH. Tf24 belimo drehantrieb mit mechanischer notstellfunktion 2,5 nm (federpacket) online kaufen, 2020. URL https://apsarosio.de/tf24-belimo-drehantrieb-mit-mechanischer-notstellfunktion-25-nm-federpacket/.

Asue. Asue - arbeitsgemeinschaft für sparsamen und umweltfreundlichen energieverbrauch e.v, 2020. URL https://asue.de/blockheizkraftwerke.

M. Barbati, G. Bruno, and A. Genovese. Applications of agent-based models for optimization problems: A literature review. *Expert Systems with Applications*, 39(5):6020–6028, 2012. ISSN 09574174. doi: 10.1016/j.eswa.2011.12.015.

André Bardow and Kai Leonard, 2018.

Belimo. Belimo: Technisches datenblatt drehantrieb trfd24-sr (-o): Stetiger drehantrieb mit notstellfunktion für 2- und 3-weg-regel-kugelhahnen, 2020. URL https://www.belimo.ch/pdf/d/TRFD24-SR(-O)_1_1_de.pdf.

BMU. Klimaschutz in zahlen: Klimaschutzziele deutschland und eu - bundesministerium für umwelt, naturschutz, bau und reaktorsicherheit, 2020. URL https://www.bmu.de/fileadmin/Daten_BMU/Download_PDF/Klimaschutz/klimaschutz_in_zahlen_klimaziele_bf.pdf.

BMWI. Hoher energieverbrauch des gebäudesektors - bundesministerium für wirtschaft und energie, 2020. URL https://www.bmwi-energiewende.de/EWD/Redaktion/Newsletter/2014/22/Meldung/hoher-energieverbrauch-des-gebaeudesektor.html.

Ibrahim Dincer, Marc A. Rosen, and Pouria Ahmadi. *Optimization of Energy Systems*. John Wiley & Sons, Ltd, Chichester, UK, 2017. ISBN 9781118894484. doi: 10.1002/9781118894484.

M. S. Elliott and B. P. Rasmussen. Neighbor-communication model predictive control and hvac systems. In *American Control Conference (ACC), 2012*, pages 3020–3025, Piscataway, NJ, 2012. IEEE. ISBN 978-1-4577-1096-4. doi: 10.1109/ACC.2012.6315308.

Engineering Toolbox. Engineering toolbox, (2003). water - thermophysical properties, 2020. URL https://www.engineeringtoolbox.com/water-thermal-properties-d_162.html.

Alfonso González-Briones, Fernando de La Prieta, Mohd Mohamad, Sigeru Omatu, and Juan Corchado. Multi-agent systems applications in energy optimization problems: A state-of-the-art review. *Energies*, 11(8):1928, 2018. doi: 10.3390/en11081928.

V.S.K.V. Harish and Arun Kumar. A review on modeling and simulation of building energy systems. *Renewable and Sustainable Energy Reviews*, 56:1272–1292, 2016. ISSN 1364-0321. doi: 10.1016/j.rser.2015.12.040. URL http://www.sciencedirect.com/science/article/pii/S1364032115014239.

Joana Hora and Pedro Campos. A review of performance criteria to validate simulation models, 2015.

Max Huber. Agentenbasierte gebäudeautomation raumlufttechnischer anlagen. 2016.

Bernardo Huberman and Scott Clearwater. *A Multi-Agent System for Controlling Building Environments*. PhD thesis, 1995.

Alexander Kümpel, Marc Baranski, and Dirk Müller. Hierarchical multi-agent control of hvac systems. 2019.

KWH Preis. Was kostet eine kilowattstunde (kwh) gas?, 2020. URL https://www.kwh-preis.de/gas/ratgeber/was-kostet-eine-kilowattstunde-gas.

Julian Lanz. *Entwciklung einer agentenbasierten Betriebsoptimierung für Gebäudeenergiesysteme*. PhD thesis, RWTH Aachen University, Aachen, 2019.

Ming-Hua Lin, Jung-Fa Tsai, and Chian-Son Yu. A review of deterministic optimization methods in engineering and management. *Mathematical Problems in Engineering*, 2012: 1–15, 2012. ISSN 1024-123X. doi: 10.1155/2012/756023.

Christian Märtel. Lohnt sich eine solaranlage? *DAA Deutsche Auftragsagentur GmbH*, 2020, 2020. URL https://www.solaranlagen-portal.com/solar/lohnt-sich-eine-solaranlage.

Petru-Daniel Morosan, Romain Bourdais, Didier Dumur, and Jean Buisson. Distributed mpc for multi-zone temperature regulation with coupled constraints. *IFAC Proceedings Volumes*, 44(1):1552–1557, 2011. ISSN 1474-6670. doi: 10.3182/20110828-6-IT-1002.00516. URL http://www.sciencedirect.com/science/article/pii/S1474667016438309.

Dirk Müller. Vorlesung 11: Kraft-wärme-(kälte)-kopplung, 2019a.

Dirk Müller. Vorlesung 3: A. v. energiewandlung. |, 2019b.

Dirk Müller. Vorlesung 8: Wärmeübertrager mit phasenwechsel, 2019c.

Brian Olson, Irina Hashmi, Kevin Molloy, and Amarda Shehu. Basin hopping as a general and versatile optimization framework for the characterization of biological macromolecules. *Advances in Artificial Intelligence*, 2012:1–19, 2012. ISSN 1687-7470. doi: 10.1155/2012/674832.

James B. Rawlings, David Q. Mayne, and Moritz M. Diehl. *Model Predictive Control: Theory, Computation, and Design*. Nob Hill Publishing, Madison, Wisconsin, 2nd edition edition, 2017. ISBN 9780975937730.

Neha Raghu Ruchika. Model predictive control: History and development. 2013.

F. Salem and M. I. Mosaad. A comparison between mpc and optimal pid controllers: Case studies. In *Michael Faraday IET International Summit 2015 (MFIIS 2015)*, IET conference publications, pages 11 (7 .)–11 (7 .), Red Hook, NY, 2016. Curran Associates Inc. ISBN 978-1-78561-186-5. doi: 10.1049/cp.2015.1607.

Gianluca Serale, Massimo Fiorentini, Alfonso Capozzoli, Daniele Bernardini, and Alberto Bemporad. Model predictive control (mpc) for enhancing building and hvac system energy efficiency: Problem formulation, applications and opportunities. *Energies*, 11(3):631, 2018. doi: 10.3390/en11030631.

Marwin Felix Spelter. *Simulationsgestützte Bewertung von Regelstrategien anhand des Energieversorgungssystems der Versuchshallo E.ON*. PhD thesis, RWTH Aachen University, Aachen, 2018.

STROM-REPORT. Strompreisentwicklung | strompreiserhöhung 2020 | strompreis, 2020. URL https://strom-report.de/strompreise/strompreisentwicklung/.

David J. Wales and Jonathan P. K. Doye. Global optimization by basin-hopping and the lowest energy structures of lennard-jones clusters containing up to 110 atoms. *The Journal of Physical Chemistry A*, 101(28):5111–5116, 1997. ISSN 1089-5639. doi: 10.1021/jp970984n.

Xin-She Yang. *Introduction to mathematical optimization: From linear programming to metaheuristics*. Cambridge International Science Pub, Cambridge, UK, 2010. ISBN 978-1-904602-82-8. URL http://search.ebscohost.com/login.aspx?direct=true&scope=site&db=nlebk&db=nlabk&AN=311051.

Appendix

A Appendix

A.1 Parameters for the Cost Function of the Sub-Coordinators

Parameter	HTS	HXS	HPS
a	10	5	20
b	6	2	6
c	10	0	20
d	6	0	6

Table A.1: Parameters for the dimension and the pre-factor of the constraint-costs of the sub-coordinators

A.2 Derivation of the Energy Balance

First, the total differential of the internal energy is established [Bardow and Leonard, 2018].

$$du(v,T) = \left(\frac{\delta u}{\delta v}\right)_T \cdot dv + \left(\frac{\delta u}{\delta T}\right)_v \cdot dT \tag{A.1}$$

The first part of the total differential A.1 is the expression of the internal pressure. The latter latter part equates to the heat capacity in isochor conditions.

$$du(v,T) = \Pi_T \cdot dv + c_v \cdot dT \tag{A.2}$$

The storage contains water, which is modeled as an ideal liquid. Therefore, water is assumed to be incompressible. For this reason, the differential dv equates to zero and the contribution of the internal pressure to the internal energy can be neglected. Consequently, the internal energy exclusively depends on the temperature and the heat capacity of its substance.

$$du(T) = c_v \cdot dT \tag{A.3}$$

Multiplying the differential of the specific internal energy with the considered mass and taking the time differential results in equation A.4. This mathematical expression builds

the foundation to quantify the relation between the time and the temperature inside of the storage.

$$\frac{dU}{dt} = m \cdot c_v \cdot \frac{dT}{dt} \tag{A.4}$$

A.3 Plots of the Heat Storage and the Cold Storage

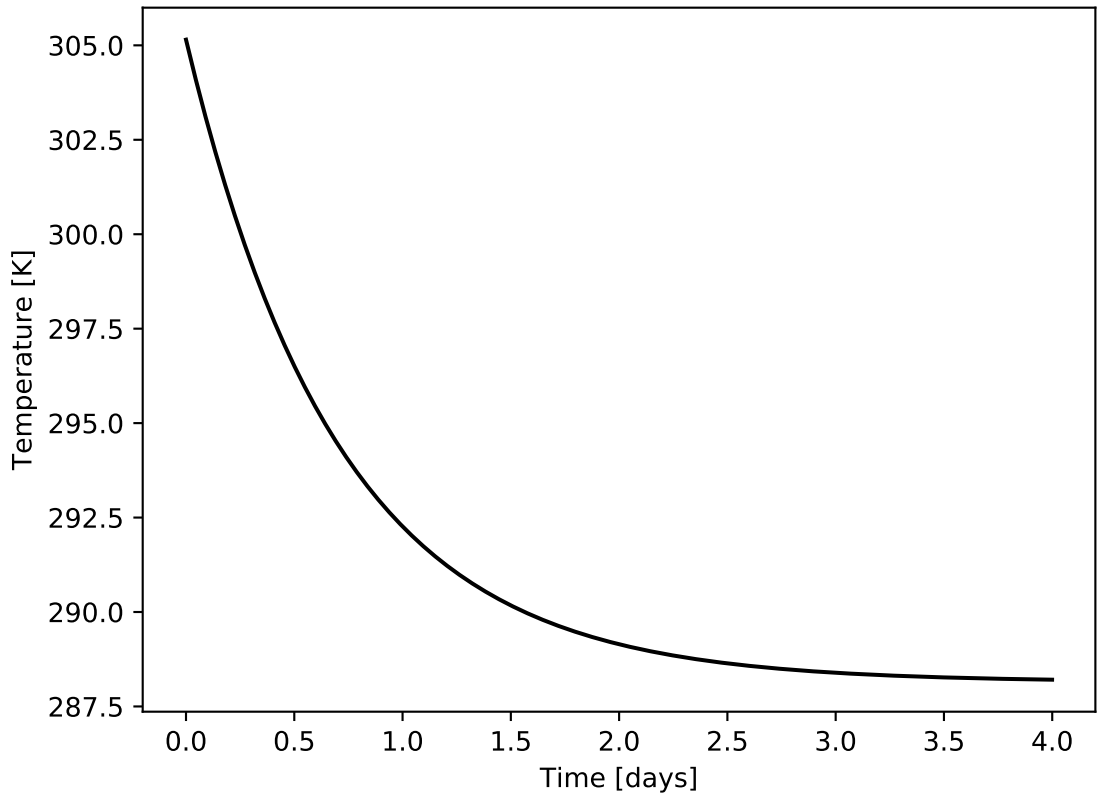

Figure A.1: Temperature profile of the heat storage to validate the chosen parameters. The thermal transmittance coefficient is chosen reasonably when the storage settles at its steady-state after approximately three days.

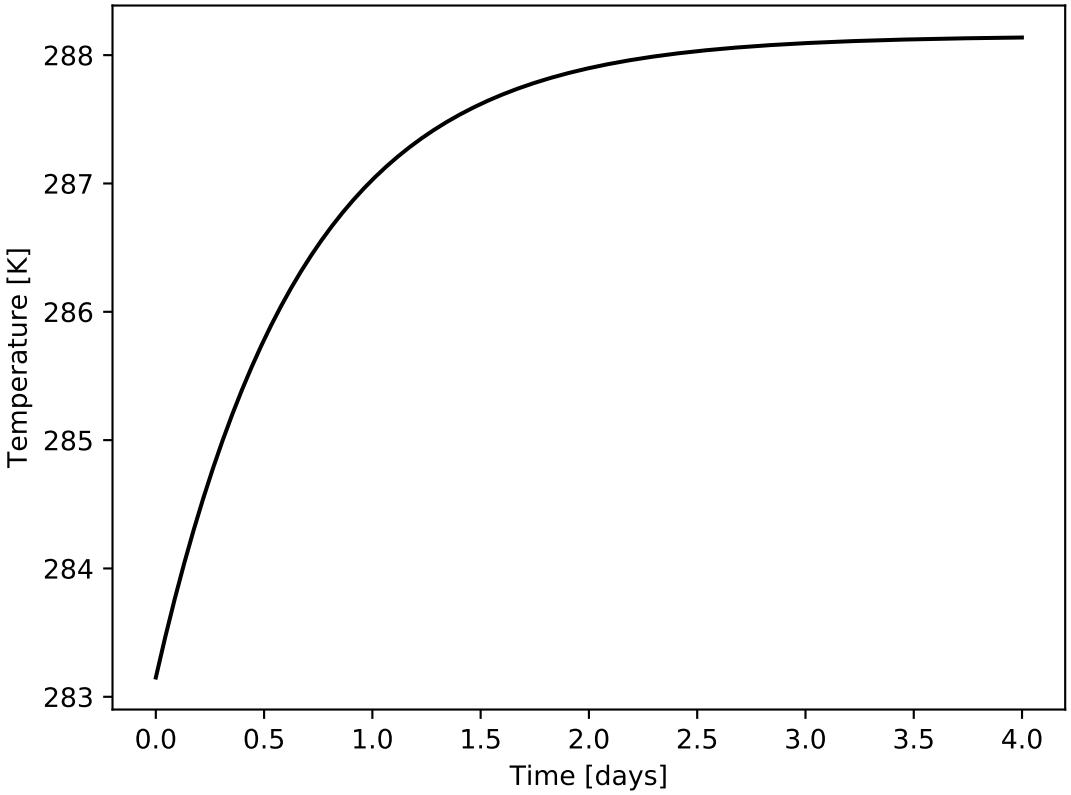

Figure A.2: Temperature profile of the cold storage to validate the chosen parameters. The thermal transmittance coefficient is chosen reasonably when the storage settles at its steady-state after approximately three days

A.4 Simulation-Parameters

Parameter	Approximated HTS	Iterative HTS	Optimized Operation	Modified Optimized Operation
$n_{iter,coor}$	10	10	3	3
$n_{iter,HTS}$	100	100	100	100
$n_{iter,HXS}$	-	-	50	20
$n_{iter,HPS}$	-	-	20	20
n_p	200	200	200	5
δT_{dev}	0,1 K	0,1 K	0,1K	2 K
δt	1.800 s	1.800s	3.600 s	3.600 s

Table A.2: Parameters for the agent-based optimization.
Abbreviations: n_{iter}: number of iterations employed by the basin-hopping algorithm, n_p: number of people affected per consumer, δT_{dev}: allowed temperature deviation, δt: duration of one time interval

Declaration of Originality

I hereby declare that this thesis and the work reported herein was composed by and originated entirely from me. Information derived from the published and unpublished work of others has been acknowledged in the text and references are given in the list of sources. This thesis has not been submitted as exam work in neither the same nor a similar form. I agree that this thesis may be stored in the institutes library and database. This work may also be copied for internal use.

Aachen, Monday 28th September, 2020

Abdullah Tokmak